Statistical modelling of air quality impacts from individual forest fires in New South Wales, Australia

Michael A. Storey[1,2], Owen F. Price[1,2]

[1]NSW Bushfire Risk Management Research Hub, Wollongong, NSW 2522, Australia
5 [2]School of Earth, Atmospheric and Life Sciences, University of Wollongong, NSW 2522, Australia

Correspondence to: Michael A. Storey (mstorey@uow.edu.au)

40

Abstract. Wildfires and controlled hazard reduction burns produce smoke that contains pollutants including particulate matter. Particulate matter less than 2.5 µm in diameter ($PM_{2.5}$) is harmful to human health, potentially causing cardiovascular and respiratory issues that can lead to premature deaths. $PM_{2.5}$ levels depend on environmental conditions, fire behaviour and smoke dispersal patterns. Forest-fire management agencies need to understand and predict $PM_{2.5}$ levels associated with a particular fire so that pollution warnings can be sent to communities and/or hazard reduction burns can be timed to avoid the worst conditions for $PM_{2.5}$ pollution.

We modelled $PM_{2.5}$, measured at air quality stations in New South Wales (Australia) from ~1400 days where individual fires were burning near air quality stations, as a function of fire and weather variables. Using VIIRS satellite hotspots, we identified days where one fire was burning within 150 km of at least one of 48 air quality stations. We extracted ERA5 gridded weather data and daily active fire area estimates from the hotspots for our modelling. We created random forest models for afternoon, night and morning $PM_{2.5}$ levels to understand drivers of and predict $PM_{2.5}$.

Fire area and boundary layer height were important predictors across the models, with temperature, wind speed and relative humidity also important. There was a strong increase in $PM_{2.5}$ modelled with decreasing distance, with a sharp increase when the fire was within 20 km. The models improve our understanding of the drivers of $PM_{2.5}$ from individual fires and demonstrate a promising approach to $PM_{2.5}$ model development. However, although the models predicted well overall, there were several large under-predictions of $PM_{2.5}$ that mean further model development would be required for the models to be deployed operationally.

1 Introduction

Smoke from forest fires produces pollutants harmful to human health, which have been linked to tens or hundreds of thousands of deaths per year globally (Chen et al., 2021; Johnston et al., 2012). Particulates smaller than 2.5 μm, i.e. $PM_{2.5}$ measured as micrograms per cubic metre of air (μgm^{-3}), are of particular concern (Haikerwal et al., 2016; Reid et al., 2016). $PM_{2.5}$ is a criteria pollutant in regulatory systems for air quality, for example, in the USA National Ambient Air Quality Standards and the Australian National Environment Protection (Ambient Air Quality) Measure.

Hazard reduction burns (HRB; a.k.a prescribed or planned burns) and wildfires can both produce high levels of $PM_{2.5}$. The impact of wildfire-produced $PM_{2.5}$ on populations, including hospitalisations and premature deaths, varies yearly and spatially depending on wildfire occurrence (Matz et al., 2020; Jaffe et al., 2008), which is driven by droughts, high temperatures and strong winds. Health costs associated with the 2019-2020 wildfires in eastern Australia were estimated to be around 2 billion dollars (Johnston et al., 2021). Massive areas burnt, including over 5 million ha burnt in the state of New South Wales alone (Filkov et al., 2020), predominantly in eucalypt forests in the mountains and coastal areas between 28 and 38 degrees south of the equator. While wildfire ignitions and sizes are unpredictable, HRBs are planned and controlled fires that are conducted to limit the spread and intensity of future wildfires by reducing fuel amounts. There have been notable instances when HRBs caused poor air quality in large cities (Broome et al., 2016; He et al., 2016; Miller et al., 2019). Large areas of land can be burnt under HRBs, for example, in Western Australia, 7 % of the forest is treated via HRBs each year (Bradshaw et al., 2018), while in Georgia, USA, 3-4 million ha are treated each year (Zeng et al., 2008). HRBs also typically occur closer to population centres (Price and Bradstock, 2013) and burn under calm, still weather conditions that may be more conducive to high pollution levels (Di Virgilio et al., 2018a). Borchers-Arriagada et al. (2021) found, by comparing population-weighted $PM_{2.5}$ exposure on days dominated by HRBs or wildfires, that HRBs in New South Wales (NSW) Australia imposed higher health costs per hectare burnt than wildfires. Further research is required but differences may stem from different fuel consumption rates (Price et al., 2022), plume behaviour and/or weather.

We need better tools to help understand $PM_{2.5}$ dispersal and air quality impacts from individual fires. Improving the tools available to forest fire management agencies would improve pollution warnings and indicate changes that could be made to HRB strategies to reduce community $PM_{2.5}$ exposure, e.g. identifying low pollution risk days to conduct HRBs. Attributes of an individual fire that could affect their $PM_{2.5}$ output and/or exposure of people to $PM_{2.5}$ are fire size, rate of heat and smoke production, fire proximity to human populations, and weather conditions including temperature, humidity, wind speed, wind direction, atmospheric stability and differences in weather between the HRB location and the $PM_{2.5}$ monitor location (Price and Forehead, 2021; Reisen et al., 2015). There is some knowledge about the influence of weather on pollution, but this has been investigated at a larger scale than individual fires. For example, days with HRBs are likely to have poorer air quality in Sydney when there are cool, stable conditions with light westerly winds (Di Virgilio et al., 2018a), while poor air quality, as

measured by ozone levels, tends to occur with a high-pressure system to the east of Sydney with light north-westerly winds and a sea-breeze (Hart et al., 2006).

There are a variety of ways to improve our understanding of $PM_{2.5}$ from individual fires. Atmospheric dispersion models can predict the spread of particulates from fires based on modelled atmospheric dynamics and are routinely used in many countries to guide burning operations and community warnings for HRBs. However, while evaluations of such systems are rare, existing evaluations indicate a poor to moderate agreement between predictions and observations (Yao et al., 2014; Saide et al., 2015), possibly because the local effects of HRBs are poorly captured by the models.

An alternative method is to relate air quality observations directly to real fires to calculate how far the smoke impact is likely to spread and under what conditions. Air quality measurements can be from ground-based stations or via satellite-based measurements, e.g. aerosol optical thickness (Gupta et al., 2007). For ground-based measurements, studies have been done using monitors stationed up to ~10 km from HRBs (Pearce et al., 2012; Price and Forehead, 2021). Pearce et al. (2012) made 684 24-hour observations of $PM_{2.5}$ by placing monitors around 55 forest HRBs. They found that $PM_{2.5}$ concentrations fell to near-background levels within 3 km of the fire perimeters. Price and Forehead (2021) made 5445 hourly observations of $PM_{2.5}$ with a combination of fixed and mobile monitors around 18 forest HRBs. They also found that $PM_{2.5}$ concentrations had largely fallen to background levels by 3 km but this depended on weather conditions. One of the HRBs caused poor air quality at monitors more than 50 km away. These studies captured the local effects of the HRBs but did not explain why HRBs can impact air quality much further away.

Deploying air quality monitors to wildfires is difficult due to the large size of wildfires, unpredictable ignition and spread and the safety risks of working near an active wildfire. However, large permanent air quality monitoring systems can be used to gather $PM_{2.5}$ data for wildfires and HRBs, for example, the NSW Air Quality Monitoring Network. Here, we use historical fire and air quality data to identify the occasions when an individual fire was burning within 150 km of a monitor in the NSW Air Quality Monitoring Network from 2012 to 2021, and develop random forest models of $PM_{2.5}$ concentrations at individual monitors as a function of fire area, distance and weather conditions. Our aims were:

1) Improve understanding of the fire and weather conditions that influence smoke dispersal and $PM_{2.5}$ levels.
2) Develop predictive models of $PM_{2.5}$ output from individual forest fires, as a complement to physical models, to improve warnings.
3) Make inferences about potential changes in HRB protocols that could reduce $PM_{2.5}$ impacts.

2. Methods

2.1 Fire Data

Our study period was from February 2012 to September 2021 because this was when our main fire data set was available (see below). For the study period, we created a spatial dataset of forest fires that were actively burning within 150 km of air quality monitoring stations (AQS) maintained by the NSW Department of Planning and Environment (DPE) (Fig. 1). 150 km captures most of the eucalypt-dominated Blue Mountains that is subject to the majority of fire activity near Sydney. We assigned

140   attributes of fire location, fire type (Hazard Reduction Burn (HRB) or Wildfire (WF)), date of fire activity and AQS name and location. Each fire had at least one active date and most burnt on several days. As a fire could be within a 150 km buffer of multiple AQS, there was a separate row in our data for each fire and AQS combination. For our modelling, we used only cases where, for each AQS and day, only one fire was active within 150 km of the AQS. We did not analyse cases where multiple fires were burning on the same day near the same AQS as it was unclear which fire produced the smoke that reached the AQS.

145   We relied on two data sources to identify fire locations, type and active dates: NSW fire history GIS polygons (NPWS, 2021), maintained by NSW National Parks and Wildlife Service (NPWS), and VIIRS SNPP hotspots, downloaded from NASA's Fire Information for Resource Management System (Schroeder et al., 2014; Nasa, 2021). VIIRS SNPP, which refers to the Visible Infrared Imaging Radiometer Suite - Suomi National Polar-orbiting Partnership, hotspots were available beginning 20 January 2012.

150   The fire history dataset is a spatial polygon dataset of the final burnt area of fires across NSW, which has attributes of fire identity (name and number), fire type (HRB or WF) and start and end dates. We did not rely solely on the fire history to identify fire locations and dates because an initial inspection suggested some issues for our analysis. These included fires identifiable from VIIRS hotspots/images that were missing from the fire history; occasional errors in the start and end date recording; the final fire polygon being the combination of separate fires that eventually merged; and the data identifying only fire start and

155   end date, not whether a fire was actively burning on each day between those dates (e.g. fires may have extinguished then reignited on different days). Also, the data did not capture daily fire progression only the final boundary, meaning the location of fire activity on the first day (perhaps a few hectares) was not well represented by the final fire polygon (perhaps tens or hundreds of thousands of hectares), which was particularly an issue for WF.

We employed a process to map active fire dates and locations from clusters of VIIRS SNPP hotspots. We used VIIRS SNPP

160   hotspots instead of MODIS as VIIRS are higher resolution (at nadir, 375 m vs. 1km for MODIS), thus can detect more hotspots per fire than MODIS, which reduces the chance that an active fire is missed (Schroeder et al., 2014). The process to create hotspot clusters for each day for each AQS was to:

1. Extract all hotspots within 150 km of the AQS.
2. To focus on forest fires, remove hotspots that were in grassland or open woodland by removing hotspots with low
165   foliage projective cover score (Gill, 2012; Gill et al., 2017). This measure of canopy density is equal to the proportion of ground that the vertically projected area of the green foliage covers. We removed hotspots with a cover fraction of less than 0.25 so that our analysis only included dense woodlands, open forests and closed forest types (Specht and Specht, 1999).
3. Buffer each hotspot by 2.5 km and dissolve overlapping buffers into a single polygon, thus creating hotspot cluster
170   polygons (Fig. 2).
4. Remove clusters that did not have at least five day or night hotspots. This was our minimum threshold for fire activity, as we wanted to exclude small fires such as burning heaps on farmland that can be detected by VIIRS. We also tested three as a minimum threshold, which produced similar but less accurate models.
5. Calculate the daily active fire area by intersecting the hotspot points in a cluster with a 500m x 500 m grid (25 ha
175   cells) covering the study area. The area assigned to each cluster was the number of unique intersecting cells x 25 ha.
6. Repeat the process for each combination of date and AQS.

Where a fire identified from the above process (a "VIIRS fire") intersected an NPWS fire history polygon between its start and end date, we assigned the fire name, number and type (HRB or WF) to the VIIRS fire. If multiple VIIRS fires intersected the same fire history polygon, we merged them into a single fire with the same attributes for analysis. If a VIIRS fire intersected multiple fire history polygons, we assigned the attributes from the fire history polygon with the largest overlapping area. NPWS fire history polygons were excluded from analysis if either the start or end date was missing, or a polygon had no intersecting VIIRS hotspots. If a VIIRS fire did not intersect a fire history polygon, we assigned the fire type based on the date: from October to February (inclusive) were WF and all other months were HRB. For each fire identified we added attributes of distance and direction from AQS to fire centroid (Fig. 2), i.e. the arithmetic mean of the hotspot coordinates, with a separate row for each fire and AQS combination (within 150 km).
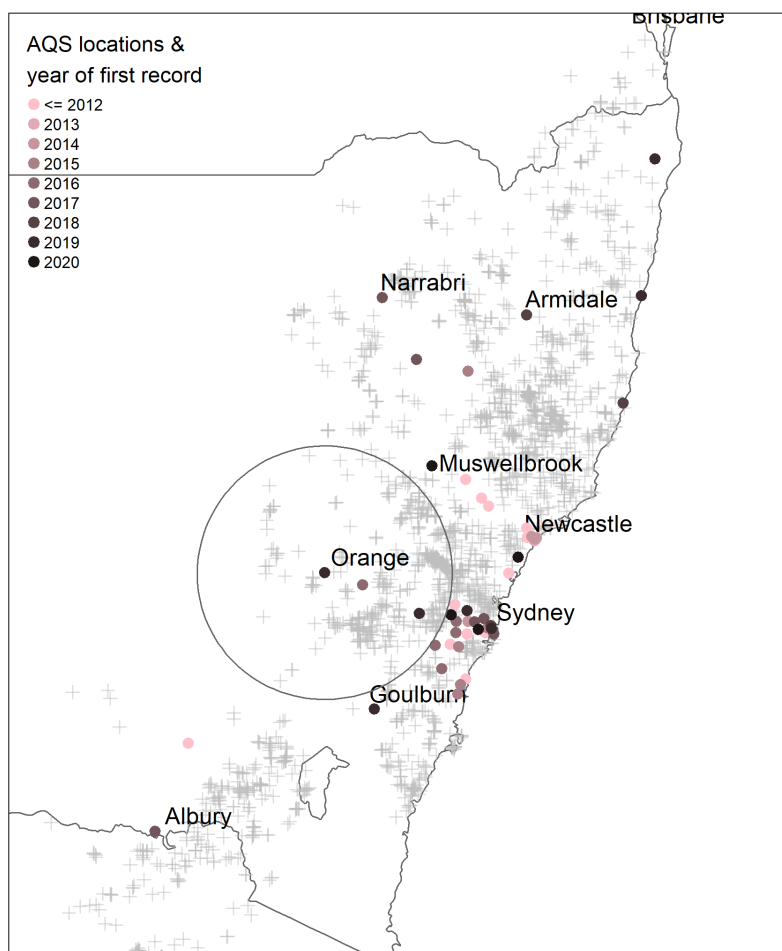
Figure 1: Map of the study area (New South Wales, Australia) showing air quality monitoring stations (AQS, n=48), coloured by year of first PM$_{2.5}$ record. Grey crosses are the locations of all fires used in analysis, with one cross per fire per day. 150 km buffer shown around Orange AQS as an example (all AQS had 150 km buffers for analysis).
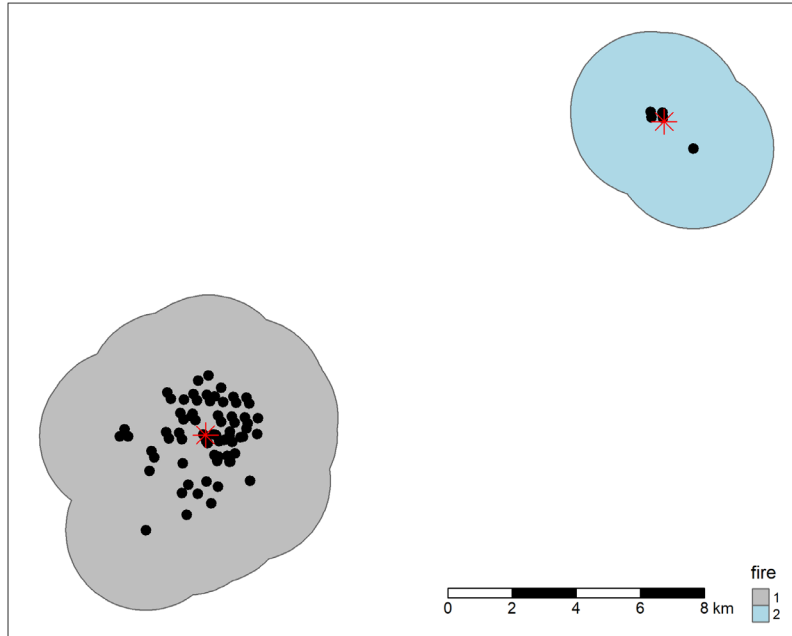
Figure 2: Example of creating clusters from VIIRS SNPP hotspots. Black dots are hotspots, red asterisks are fire centroids, i.e. the arithmetic mean of the hotspot coordinates. The image has two separate fires. Each hotspot is buffered by 2.5 km, with all overlapping buffers merged and hotspots given separate identity numbers based on which final buffer they fell within. Two separate fires are created here because of distinct fires where buffers don't overlap, i.e. greater than 2 buffer widths (5 km) apart. Fire 1 (grey) has > 50 hotspots, fire 2 (blue) has 5 hotspots. Note that fire area used in analysis was calculated via an intersection with a 500 m x 500 m grid, not buffer size (see methods).

2.2 PM$_{2.5}$ Data

We modelled PM$_{2.5}$ (μgm^{-3}) as a function of several environmental predictors. We downloaded all available PM$_{2.5}$ data (hourly averages) from the NSW DPE for the period 2012 – 2021, which comprised 48 AQS. Data were available free online at https://data.airquality.nsw.gov.au/docs/index.html. We calculated mean PM$_{2.5}$ for each AQS for three six-hour periods:

1. **Afternoon**: 1400 to 1900 AEST inclusive. This period covered peak burning conditions in the afternoon and after sunset, although sunset and fire ignition times varied.
2. **Night:** 2100 to 0200 AEST inclusive. Covered the night period starting on the same day as the fire.
3. **Morning:** 0500 to 1000 AEST inclusive, next day after fire day. Captured early next morning conditions after the main periods of fire activity are likely to have ended, although some fires may have burnt through the night and smoke may still have lingered.

Note that there were some missing PM$_{2.5}$ values in the data, which meant some summary afternoon/night/morning values had < six records. However, > 98 % of records were summarised from >= four hourly PM$_{2.5}$ values.

We chose these times to represent different periods in the daily cycle that may have distinct smoke, weather and fire behaviour characteristics. All fires identified in the hotspot analysis were matched to AQS summary PM$_{2.5}$ for active days when the fire

was within 150 km. Not all AQS had records for all years, as some were not operational until later in the study period (Fig. 1).

215   Note that we modelled $PM_{2.5}$ observed at air quality stations, which would include primary and secondary $PM_{2.5}$. Secondary $PM_{2.5}$ can be formed via atmospheric chemistry processes that transform emitted gases into particulates, with the processes influenced by factors including season, solar radiation, temperature and relative humidity (Fine et al., 2008; Cope et al., 2014).

2.3 Predictor variables

220   We sampled hourly weather variables at each AQS and each fire centroid from ERA5 weather grids, which is an atmospheric reanalysis product with multiple weather variables and atmospheric levels available at 30 km spatial and hourly temporal resolution (Hersbach, 2021b, a) (Table 1). We calculated the mean weather values for both surface and upper atmospheric conditions (Table 1) for the afternoon, night and morning periods as described for $PM_{2.5}$. We calculated additional variables describing the spatial relationship between the fire and each AQS. We used the AQS to fire direction and wind direction to

225   calculate the percent of time-period where the surface wind was blowing directly to the AQS, with directly meaning ±22.5 degrees of the AQS-to-fire bearing. We also used the daily active fire area based on the intersection of hotspots and a 500 m by 500 m grid (area = N intersecting cells x 25 ha), as a predictor. We included a month variable (i.e. month of the active fire date) as a predictor variable to account for any seasonal variation in background $PM_{2.5}$ levels. Month was represented as a cyclic variable, where the sine and cosine of the month (1-12) were both included in the modelling. We included the latitude

230   and longitude of the AQS to account for spatial dependence, and fire type as a factor variable to account for differences not captured by the weather/fire area variables. We also experimented with making separate models for each fire type (HRB model and WF model) for each time period but found that resulting accuracy statistics on the training and test sets were similar, so instead just used one model for each time period with fire type as a factor variable.

235

240

245

250

255

Table 1: Predictor variables used for random forest modelling. Letters mean that for the random forest modelling, weather variables were sampled at the fire (F), at the AQS (A) or both (FA). MSLP and wind speed (850 hPa) at the AQS were excluded due to being highly correlated with the same variable at the fire.

Type	Name	Units	Details
ERA5 weather	**PBLH** – Planetary boundary Layer Height (FA)	metres	Mean height of planetary boundary layer from surface, from ERA5 grids.
	MSLP – Mean Sea Level Pressure (F)	hectopascal	Mean sea level pressure of atmosphere on surface per unit area from ERA5 grids.
	WS – Wind speed (FA)	km h^{-1}	Mean wind speed 10 m above surface calculated from U and V ERA5 wind component variables.
	RH – Relative humidity (FA)	%	Mean relative humidity calculated from temperature and dew-point ERA5 variables.
	Temperature (FA)	celsius	Mean temperature 2 m above surface sampled from ERA5 grids.
	WS 850 hPa – Wind speed at 850 hPa (F)	km h^{-1}	Mean wind speed at 850 hPa calculated from U and V ERA5 pressure-levels wind component variables.
	Direct wind (FA)	%	Percent of hours during a period (afternoon etc.) where 10 m wind was blowing directly toward AQS, i.e. within a 22.5-degree arc either side.
Fire	**Fire area**	hectares	Daily active hectares calculated from the intersection of VIIRS hotspot (day and night) with a 500 m by 500 m grid (N intersecting cells x 25 ha).
	Fire Type	WF or HRB	Wildfire or hazard reduction burn

		sine, cosine	Month included to account for seasonal variation in background $PM_{2.5}$. Included as a cyclic variable: cosine and sine of integer month as separate variables.
Temporal	**Month**		
	Distance	km	Kilometres from the fire centroid (i.e. geometric centre of a hotspot cluster) to the AQS
Geographic	**AQS coordinates**	Latitude, Longitude	Coordinates of air quality monitoring stations, to account for spatial dependence.

2.4 Random Forests Modelling

Our data consisted of three separate tables (afternoon, night and morning data tables) for three models. In each table, there were 11187 rows with unique combinations of fire, AQS and date. For each fire, there could be multiple active dates and each fire could be associated with more than one AQS (i.e. it was within 150 km of multiple AQS). Our data had 48 different AQS and 1429 different days with at least one active fire near an AQS. There were 1883 different combinations of fire and day (we refer to these combinations as "fire-days") consisting of 727 fire-days that had VIIRS hotspots and a fire history record and 1156 fire-days that had only VIIRS hotspots. The fire-days from solely VIIRS hotspots were on average smaller than the fire-days with a matching NPWS fire history record (209 ha vs 854 ha respectively). 1182 fire-days were from HRBs (mean daily active fire area = 254 ha) and 701 were from WFs (mean daily active fire area = 802 ha). Each fire was observed at a minimum of one AQS, with a mean of six AQS and a maximum of 35 AQS associated with a single fire.

We trained a random forest model using the "ranger" package in R (Wright and Ziegler, 2017). Random forests are robust and efficient machine learning algorithms that involve fitting and averaging of randomized decision trees and have been applied to a range of environmental research problems including fire and emissions (Biau and Scornet, 2016; Hu et al., 2017; Shah et al., 2022). We chose random forests due to several advantages that include high accuracy, fast computation times, easy implementation, robustness and greater interpretability (compared to "black-box" methods) via simple methods to extract variable importance and partial dependence (Rodriguez-Galiano et al., 2015; Biau and Scornet, 2016; Wright and Ziegler, 2017).

We split each of our datasets into training (75 %) and test (25 %) sets for analysis, stratified by fire type so that an even proportion of HRBs and WFs appeared within each of the sets. We trained the models using the training set data and used out-of-bag (OOB) predictions vs observations for model accuracy checks and predicted to the test set to calculate test set accuracy statistics. Our accuracy statistics were the correlation coefficient (r), normalised mean error (NME) and normalised mean bias (NMB), as recommended by Emery et al. (2017) for assessing model performance. We ran three different models, one for each analysis period: 1) afternoon mean $PM_{2.5}$, 2) night mean $PM_{2.5}$, and 3) morning mean $PM_{2.5}$. Predictor variables were the weather variables in Table 1 sampled at both the AQS centroid and fire centroid, distance, daily active fire area, month and

AQS coordinates. As highly correlated variables can introduce bias into random forests variable importance calculations (Strobl et al., 2008), we removed variables from analysis where the Pearson correlation was above 0.8: MSLP at AQS and wind speed 850 hPa at AQS were excluded, each of which was correlated with the version sampled at the fire.

We assessed the variable "permutation" importance using the ranger package. Permutation importance is derived from a process where reduction in model accuracy on OOB predictions is calculated after randomly shuffling values for each variable, calculated for all trees and variables (Wright et al., 2016). We assessed predictor variable effects using partial dependence plots calculated in the "pdp" package in R (Greenwell, 2017), and by creating prediction plots where $PM_{2.5}$ was predicted with all variables held at mean values except two variables of interest, which were each assigned three different levels to illustrate their effects. We also conducted a short descriptive analysis, using satellite images and hourly $PM_{2.5}$ of large outliers in the models to understand potential reasons for inaccurate predictions. This is included in Appendix A.

2.5 Limitations

There are several limitations to our methods that should be considered when interpreting the results. Our process to identify active fires from VIIRS hotspots excluded hotspots that were outside the 150 km AQS buffer, even if they were part of a fire that straddled the buffer edge. There may be occasions where smoke from hotspots, and entire fires, from > 150 km reached an AQS and influenced $PM_{2.5}$, e.g. large WFs during the 2019-20 "Black Summer". The effect of such fires was not captured in our methods.

We set a minimum fire activity threshold of five hotspots (day or night). This may mean that days recorded as having only one fire may have had other smaller fires in the area that may have produced smoke that affected $PM_{2.5}$. Relying on VIIRS had the advantage of being able to better detect when a fire was active, but our process may not have captured all fires on any given day due to cloud cover impeding VIIRS hotspot detection. This may be a form of bias in our analysis as the cloudiest days were selected against. Additionally, VIIRS SNPP hotspots are acquired early afternoon and early morning, meaning that the total burnt area on a day is not measured, only the active area at the time of VIIRS acquisitions. Fire area, or the number of fires, may have been underestimated if clouds were impeding hotspot detection. Our decision to analyse only days with one fire, to better understand distance and direction variables, means that there is a selection bias against the most active fire days (i.e. days with multiple fires). This may include the worst WF days, where multiple fires were more likely to ignite, particularly during 2019-2020. For days that are most suitable for HRBs, authorities are more likely to ignite multiple HRBs. Such days, which could include the worst pollution events, were not included in our analysis but were the subject of separate research (Storey and Price, 2022).

Note that in our VIIRS hotspots clustering process, we used a buffer of 2.5 km to provide a broad "search" area in which to group hotspots: any hotspots within 5 km of each other (two buffer widths) or less would be grouped. This may have meant that on some occasions, separate small fires were grouped. However, we deemed it reasonable to treat these as one fire for our purposes given the similar location meant smoke would be travelling along the same general bearing towards an AQS, which

was important for the direct wind variable (Table 1). For example, two fires 5 km apart would have a ~3 degree difference in bearing to an AQS 100 km away (~5 degrees at 50 km). Smaller or larger buffers may have produced different results.

3. Results

3.1 Variable summaries

Plots of the distribution of $PM_{2.5}$ and predictor variables are shown in Figure 3. $PM_{2.5}$ was skewed toward low values (afternoon, night, morning mean = 8.1, 10.7, 10 μgm^{-3}), with occasional very smoky periods (afternoon, night, morning maximum = 294.2, 394.8, 506.2 μgm^{-3}). Most fires were between 75 and 150 km from the monitoring stations and only 20 % of fires had their closest AQS within 50 km. Daily active fire area derived from VIIRS hotspots was heavily skewed toward lower values (mean = 458 ha, 95th centile = 1175 ha). The maximum fire area was 31800 ha, < 1 % of fires (all WF) were over 10000 ha and 94 % were less than 1000 ha.

Afternoon conditions were generally hotter, less humid and had higher PBLH at both fire and AQS locations than nights and mornings. Between WF and HRB, WF afternoons were hotter, drier and had higher PBLH (Fig. 3). MSLP was similar between afternoon, night and morning, but skewed lower for WF compared to HRB. The wind direction variables were clustered around zero, indicating that most of the time wind at the fire and at the AQS was not moving smoke directly from the fire to the AQS (Fig. 3). For example, only 5 % of rows in the afternoon data indicated that wind sampled at the AQS was coming directly from the fire for at least 3 of the 6 hours. For wind sampled at the fire, this figure was 11 %.
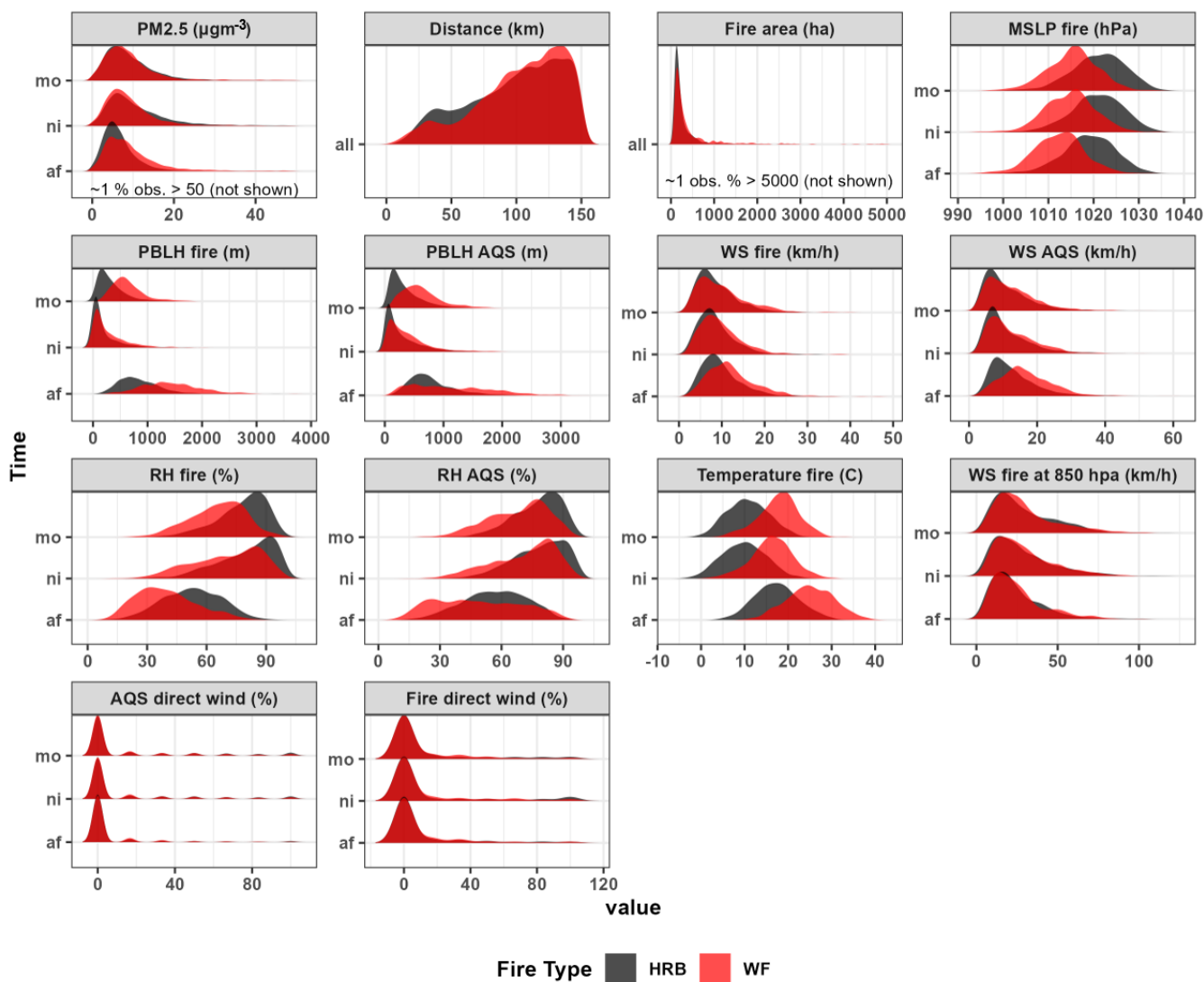
335 **Figure 3: Distribution of PM$_{2.5}$ and predictor variables used in random forest modelling, excluding latitude, longitude, fire type and month. Distance and daily active fire area are daily variables, so are identical for afternoon, night and morning model datasets. Distributions for at-fire variables from unique fire-day combinations, for at-AQS variable values are from unique AQS-day combinations. af=afternoon, ni=night, mo=morning. AQS=Air Quality Station, RH=Relative Humidity, WS=Wind Speed, PBLH=Planetary Boundary Layer Height, MSLP=Mean Sea Level Pressure.**

340 **3.2 Highest PM$_{2.5}$ days**

Figure 4 shows the 20 highest mean PM$_{2.5}$ values for each six-hour period for HRBs and WFs. The top PM$_{2.5}$ values were much greater for WFs than for HRBs in the afternoon, night and morning (~150 to 200 µgm^{-3} greater for each). >= 80 % of

the top 20 PM$_{2.5}$ values for WF for afternoon, morning and night were associated with the 2019-2020 wildfires in NSW, many with the Gosper's Mountain wildfire in the Blue Mountains (Boer et al., 2020).

345   The top seven afternoon peaks for WF were > 100 µgm^{-3} (max= 294 µgm^{-3}) but only two of the afternoon HRB peaks were > 100 µgm^{-3}. In the night and morning, there were fewer values > 100 µgm^{-3}, but larger maximums were recorded for HRB and WF for each period (compared to the afternoon). For each rank position, WF values were greater than HRB values, except in the night model where from positions 3 to 20, the HRB values were higher. More information, including satellite images, weather plots and descriptions, on the conditions surrounding the worst PM$_{2.5}$ events for each time period for HRBs and WFs

350   is included in Appendix A.
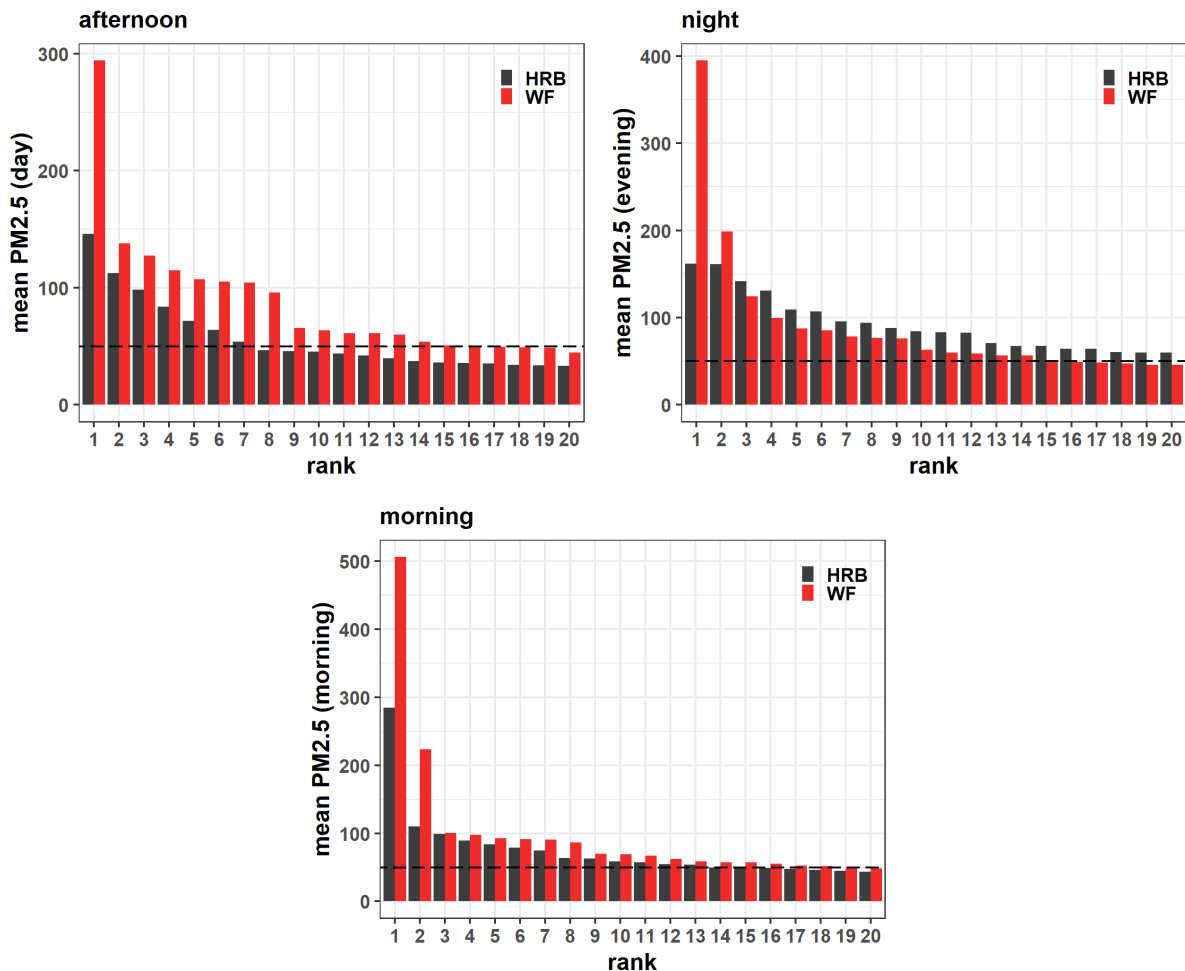
Figure 4: Highest mean PM$_{2.5}$ values for each six-hour time period for HRBs and WFs. Only the top values for each date are shown. This means if the second highest value was over 100 for a particular date at another AQS, it is not included here. The dashed line
355   **indicates 50 µgm^{-3} for reference between the three plots. Note that our data only includes situations with one fire within 150 km of an AQS for a particular date.**

3.3 Model results

Daily active fire area, PBLH (fire and AQS), temperature and RH at the fire were among the most important variables in the three models (Fig. 5). Some variables were among the most important in only one or two of the models: wind speed at the fire
360 was the fourth and fifth most important in the night and afternoon models but ninth most important in the morning model. The direct wind variables, distance to fire, AQS coordinates, MSLP, month and fire type were all of moderate to lower permutation importance in each model.

Partial dependence plots (Fig. 6) indicated that for all models, there was a sharp increase in predicted $PM_{2.5}$ when the AQS-to-fire distance was below $\sim$ 20 km, with the morning model displaying the sharpest rise in $PM_{2.5}$ as the distance decreased. This
365 effect is despite distance being of middle to lower permutation importance (Fig. 5). Partial plots indicated $PM_{2.5}$ increased as fire area increased, particularly in the 0 to 2500 ha range, which is where most training observations were situated (Fig. 3). There was a very large $PM_{2.5}$ increase above 10000 ha in the morning and afternoon models, although there is uncertainty here due to a small number of training observations > 10000 ha (Fig. 3). The shape of the PBLH effect differed for each model between the fire PBLH and AQS PBLH. At the AQS, there was a strong negative effect of PBLH (lower PBLH = higher
370 $PM_{2.5}$), particularly in the night and morning models. At the fire, each model had peak $PM_{2.5}$ at low and high values of PBLH. For the night and morning models, $PM_{2.5}$ peaked when fire PBLH was $< \sim$ 200 m, with a smaller rise $> \sim$ 800 m. For the afternoon model, the largest peak was when fire PBLH was high ($> \sim$1500 m), with a smaller rise when $< \sim$ 500 m. For RH at the fire, predicted $PM_{2.5}$ below $\sim$ 50 % RH was much higher than when RH was above 50 % in the morning and night models. For wind speed, effects varied between the fire and AQS and with the time period: lower wind speed at the AQS was associated
375 with higher $PM_{2.5}$ in all models but at the fire low and high (particularly for the night model) wind speeds were associated with higher $PM_{2.5}$.

We calculated model accuracy statistics for the training set (OOB predictions) and the independent test sets and for HRB and WF subsets of each. From the combined statistics, Pearson correlations between predictions and observations (r) for training and test sets ranged from 0.67 to 0.83 (Table 2, Fig. 7). For the statistics by fire type, r was higher for WF than for HRB. For
380 WF, r was 0.7 to 0.88 on the training and test sets. For HRBs, r was 0.59 to 0.69 on the training and test sets. NME for all combinations of training/test set and fire type ranged between 33 % and 39 %, with the lowest NME for the WF subset from the afternoon model ($\sim$33 % for training and test set). The NBE indicated that generally there was a slight over-prediction bias that ranged from $\sim$1 % to $\sim$2 %, with a maximum of 6.95 % for WF for the night model test set. The night model had under-prediction bias for HRBs on the test set (Table 2, Fig. 7).
385 The models had large under-predictions for the largest $PM_{2.5}$ values and a few large over-predictions (Fig. 7). NBE calculated on data that included only where observed $PM_{2.5}$ was >= 20 μgm^{-3} was -30.9 % (training) and -32.8 % (test) for the afternoon model, -34.5 % and -35.8 % in the night model and -29.6 % and -32.3 % in the morning model, indicating under-prediction bias for the larger $PM_{2.5}$ values. For predictions to the test set, in the afternoon model 9 observations were under-predicted by at least 30 μgm^{-3}; 4 from WF and 5 from HRB. The maximum over-prediction was by 36 μgm^{-3}. For the night model, there

390 were 15 occasions where the model under-predicted in the test set by at least 30 μgm^{-3} (12 were HRB). The maximum over-prediction was by 57 μgm^{-3}. The morning model had 14 under-predictions on the test set by at least 30 μgm^{-3}, with the largest under-prediction by 175 μgm^{-3} for a 2019-2020 WF, although the model correctly predicted this morning as having the highest PM$_{2.5}$ in the test set (observed=390 μgm^{-3}, predicted=215 μgm^{-3}). There were 3 over-predictions by at least 30 μgm^{-3}.

We explored the influence of distance and some selected variables with a series of prediction plots (Fig. 8). PM$_{2.5}$ was predicted
395 to increase substantially with decreasing distance within the first 20 km of the fire in all combinations of area, PBLH, RH and temperature in Figure 8. Beyond ~30 km there was minimal to no effect of distance, except in the morning model with a large fire area (Fig. 8a). The effect of temperature at the fire differed between models, such that as temperate increased from 10 to 25 C, PM$_{2.5}$ was predicted to decrease in the morning model but increase in the afternoon model. The plots also suggest there is generally a small difference between predicted mean PM$_{2.5}$ for WF and HRB for each model once the other predictors
400 including fire area are controlled for.
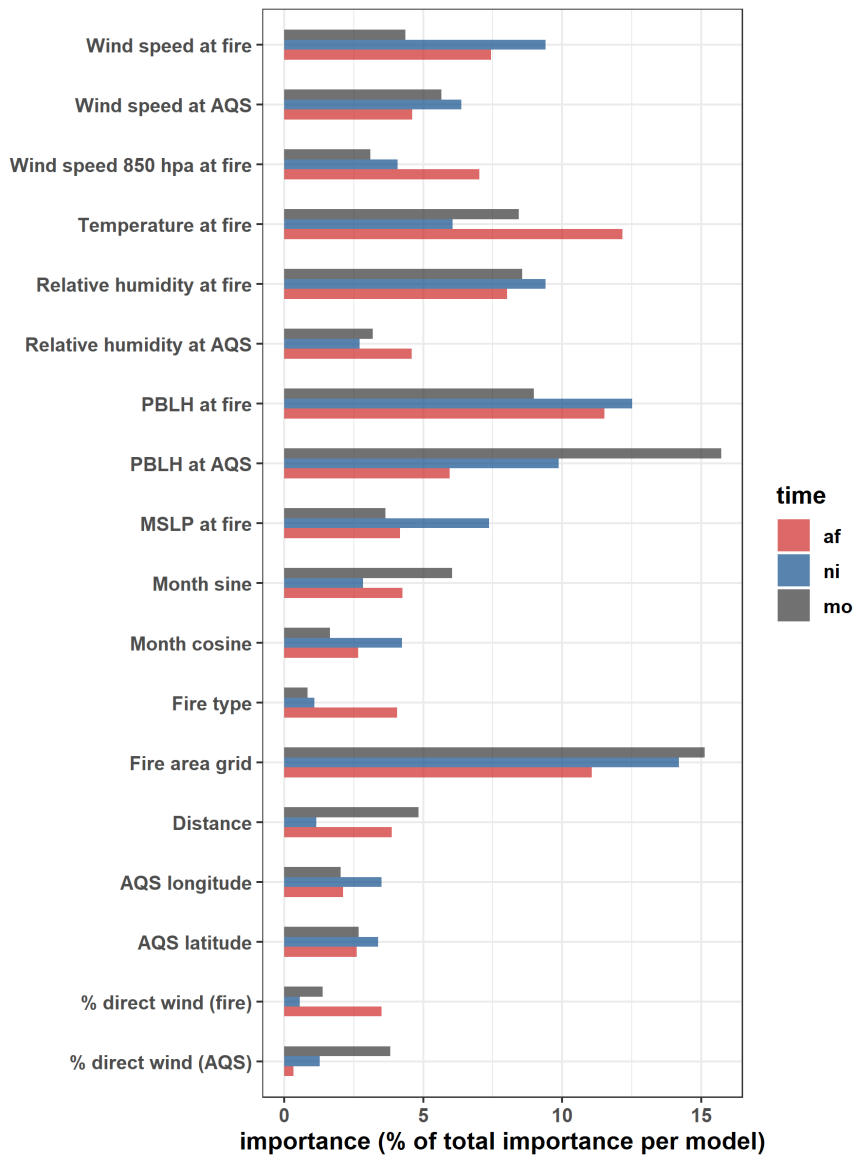
Figure 5: Variable importance for each model. A common x scale was assigned for clarity, which is the % of the total permutation importance attributable to each variable (i.e. importance/sum(importance)*100).

405
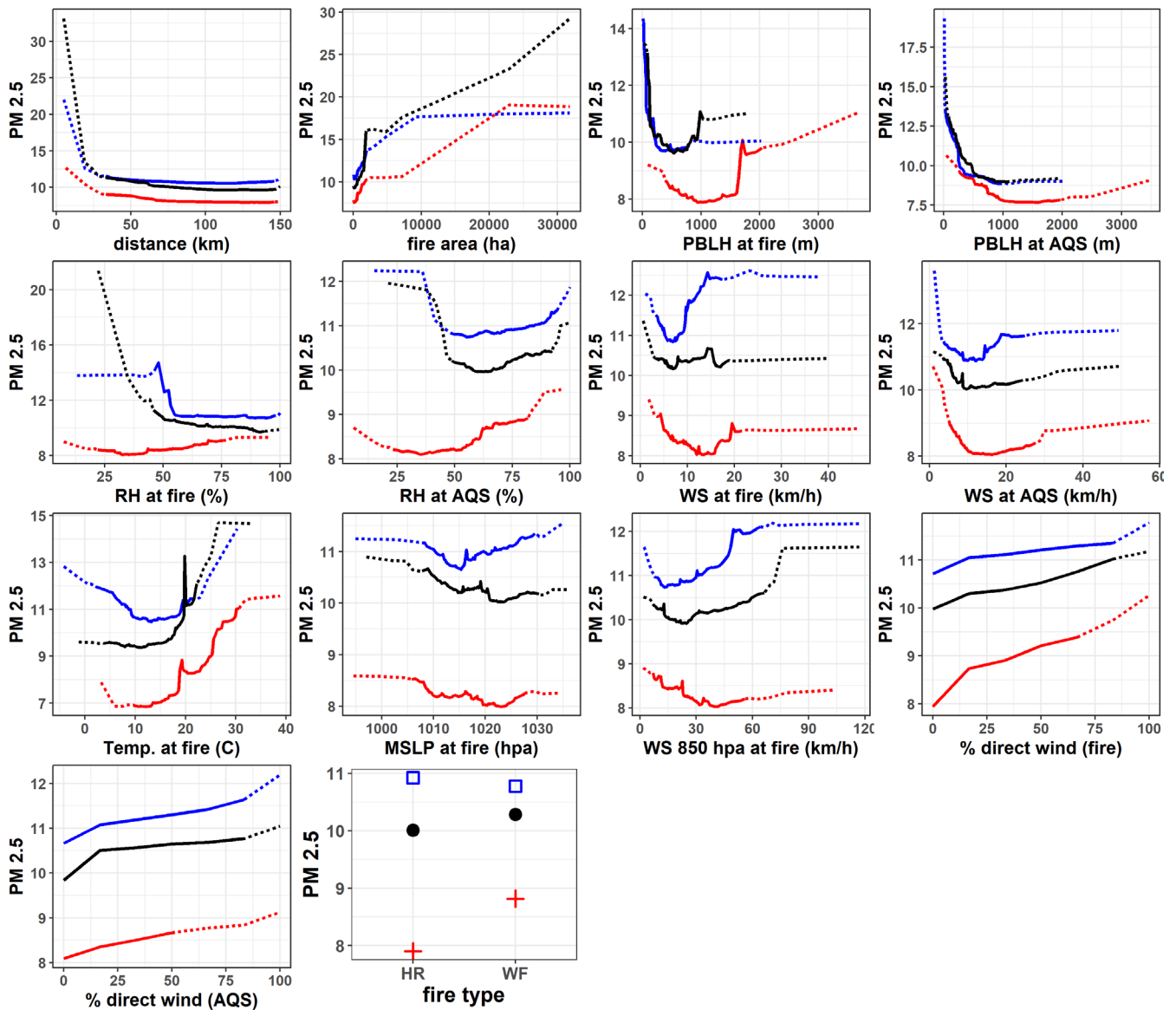
Figure 6: Partial dependence plots for the afternoon (red), night (blue) and morning (black) models. Dotted parts of lines are minimum to 5th centile and 95th centile to maximum values for each predictor variable, calculated from the training data. Where dotted parts are long, this indicates a large range of values with a small number of observed points for model training.

410

415

Table 2: Accuracy statistics from random forest modelling for training (bold) and test (in brackets) sets. Training set predictions are on out-of-bag samples during model fitting and test set predictions were made to the independent test set. Overall statistics, along with statistics on HRB and WF portions of the data are shown. *r* **= Pearson correlation, NME = Normalised mean error, NBE = Normalised bias error (Emery et al., 2017).**

		r	NME %	NBE %
Combined	Afternoon	**0.75** (0.78)	**35.5** (36)	**1.34** (1.06)
	Night	**0.67** (0.70)	**37.3** (36.5)	**1.51** (0.62)
	Morning	**0.76** (0.83)	**37.4** (37.6)	**2** (1.9)
HRB	Afternoon	**0.60** (0.69)	**37.6** (38.6)	**1.81** (1.53)
	Night	**0.63** (0.68)	**38.1** (36)	**0.81** (-2.25)
	Morning	**0.59** (0.65)	**37.9** (38.5)	**2** (2.4)
WF	Afternoon	**0.79** (0.81)	**33.1** (32.9)	**0.78** (0.51)
	Night	**0.7** (0.76)	**36** (37.5)	**2.86** (6.95)
	Morning	**0.82** (0.88)	**36.6** (36.2)	**2** (1.2)
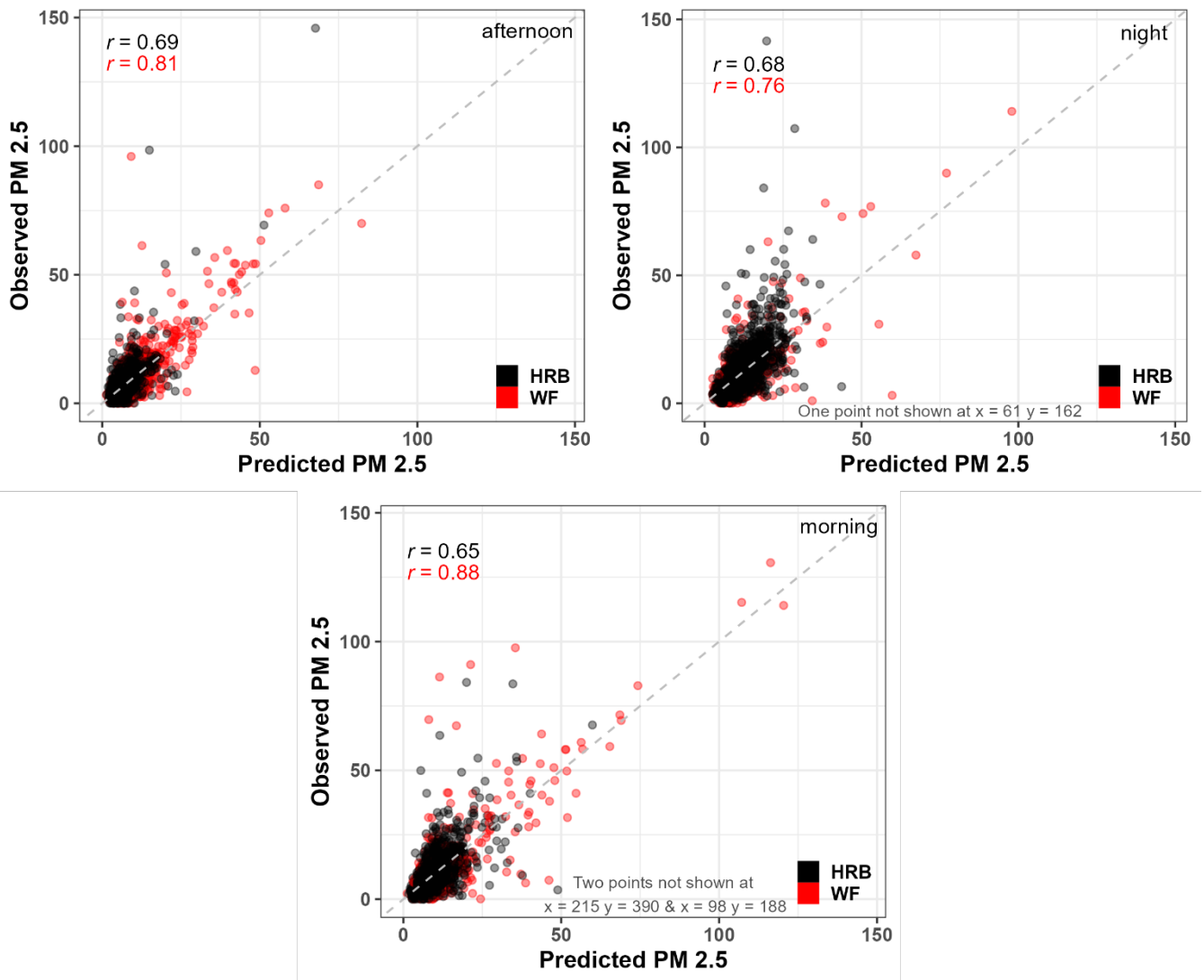
Figure 7: Predictions of each model to test set, with points coloured by fire type. Pearson correlation of predictions to observations by fire type shown in text (*r*).

425
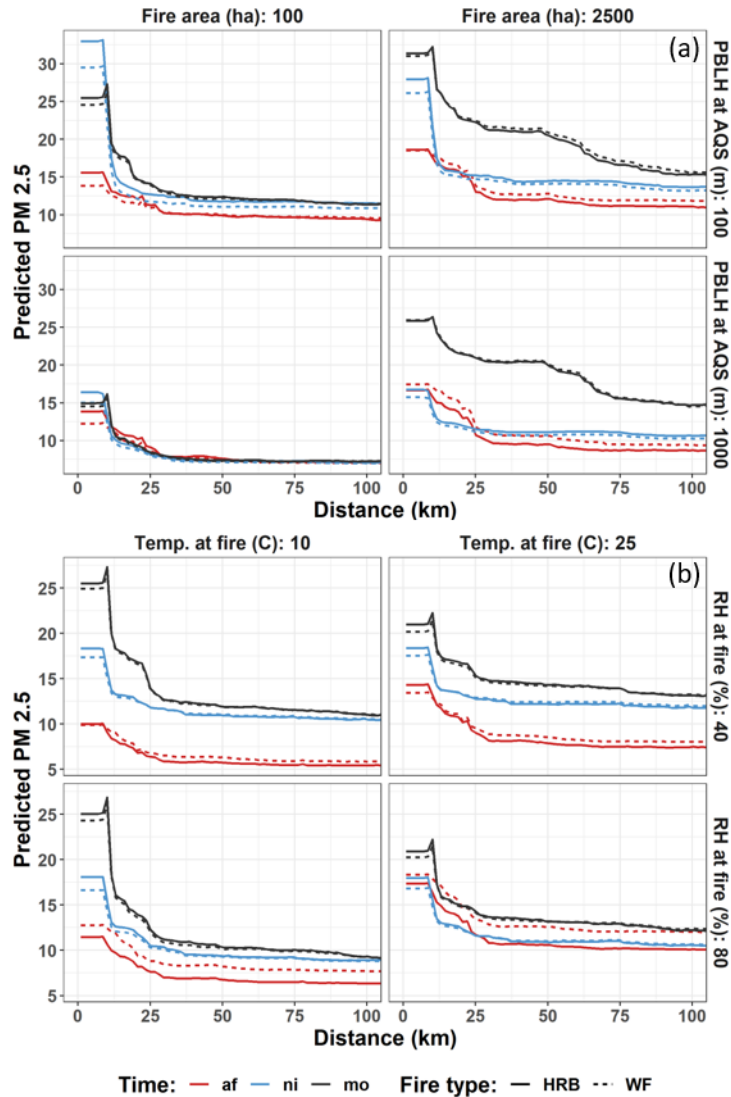
Figure 8: Predicted effects of selected variables on mean PM2.5. Colours are time periods, line types are fire types and grid squares are combinations of the daily active fire area and planetary boundary layer height at the air quality monitoring station (a) and relative humidity and temperature at the fire (b).

4. Discussion

Using empirical fire and air quality monitoring station data, we identified important drivers of particulate pollution associated with individual forest fires. The results are important in the context of our first research aim, which was to ***improve understanding of the fire and weather conditions that influence smoke dispersal and PM2.5 levels***. In our models, daily active fire area, PBLH, temperature, relative humidity and wind speed were all important drivers of PM2.5 from individual fires. The importance of these variables at the fire or at the AQS varied between models. Distance to fire generally had low permutation

importance, possibly due to the low number of AQS in the 0 to 50 km range (Fig. 3, Fig. 6). However, partial plots and prediction plots indicated a large influence on model predictions. For example, partial and prediction plots suggested that within 20 km of a fire, $PM_{2.5}$ levels rose steeply with decreasing distance. The effect of distance > 50 km was negligible in

440   most cases, suggesting other factors are more important drivers at such distances, although under certain conditions there could be raised $PM_{2.5}$ at long distances, such as with higher fire area in the morning model (Fig. 8). Based on Reisen et al. (2018), a 1000 ha prescribed burn will emit 160 tonnes of $PM_{2.5}$, enough to fill to exceedance level a cylinder capped by a planetary boundary layer of 500 m to a radius of 64 km. This means there are sufficient particulates available for a distance effect to occur should the weather conditions suit. Other authors have found similar variables to be important in modelling $PM_{2.5}$,

445   including fire size and distance when $PM_{2.5}$ was measured within ~10 km of HRBs (Pearce et al., 2012; Price and Forehead, 2021). PBLH was also a consistent predictor of $PM_{2.5}$ levels at multiple stations in Sydney during HRB days (Di Virgilio et al., 2018b). However, studies such as these have modelled $PM_{2.5}$ over smaller scales than we did here or did not attempt to link individual fires to $PM_{2.5}$ records. Our data included $PM_{2.5}$ measurements up to 150 km from a fire and we built $PM_{2.5}$ models using a much larger dataset of fires and $PM_{2.5}$ records, which here were from pre-installed permanent AQS. Therefore,

450   the results from our study are more applicable to the individual fire and $PM_{2.5}$ relationship across large geographical areas than other studies.

Our models suggest the area potentially affected by $PM_{2.5}$ from fires is larger than in Price and Forehead (2021), where raised $PM_{2.5}$ levels were mostly modelled to be within 5 km of HRBs. Here, our models suggested that raised $PM_{2.5}$ levels mostly occurred within 20 km of a fire. Our dataset includes a larger set of fires and includes WFs, which are likely to produce smoke

455   that travels further. In some individual cases in our raw data, fires caused high $PM_{2.5}$ levels > 100 km away (e.g. Appendix A Fig A3). Although relatively sparse, analysis using the more remote AQS network is more suited to detecting these longer-range effects than when monitors are placed only close to a fire.

Our second aim was ***to develop predictive models of $PM_{2.5}$ output from individual forest fires, as a complement to physical models, to improve warnings***. There was some success here: r on the test sets indicated moderate to good agreement between

460   predictions and observations: 0.78, 0.70 and 0.83 for the afternoon, night and morning models respectively. The models fit better on the WF portion of the test data (r 0.76 to 0.88) than for HRBs (r 0.65 to 0.69). The better results for WF suggest the models may be more applicable to WFs, e.g. for the issuance of pollution warnings due to WF smoke, rather than for assisting with HRB planning. An important consideration for using the models for prediction is their accuracy on the largest $PM_{2.5}$ observations. Events with very high $PM_{2.5}$ have the largest health impacts and are therefore the most important to predict, for

465   example, to correctly issue warnings or defer HRBs due to high pollution risk. Our results suggest that, while some predictions for the largest $PM_{2.5}$ observations were relatively accurate, the models did not consistently predict larger $PM_{2.5}$ events, so may not be suitable as an operational prediction tool without further development.

There are several possible reasons for the biggest outliers and limited accuracy. The AQS network is relatively sparse, being concentrated in greater Sydney, making the distance between any fire and AQS usually large. The mean distance to the closest

470   AQS for each fire-day was 88 km (10th centile = 31 km). This may partly explain why we did not detect wind direction effects.

Price et al. (2012) also did not find significant effects of wind direction when modelling $PM_{2.5}$ in relation to MODIS hotspots at similarly broad scales around Sydney and Perth. In contrast, two empirical studies that did detect clear wind direction effects from HRBs, Pearce et al. (2012) and Price and Forehead (2021), placed $PM_{2.5}$ monitors close to HRBs, mostly within ~10 km. The large distances in our data mean smoke was subject to broader weather circulation patterns before reaching an AQS, such as shown in Appendix A. This could create a varying lagged pollution effect that we did not completely account for in our modelling, because smoke may take different amounts of time to reach an AQS depending on circulation patterns. Although we did not focus exclusively on coastal areas, many AQS were in coastal areas, so may have been affected by complex wind patterns. The Sydney basin, for example, can be affected by westerly terrain-related drainage flows, sea breezes and their interaction (Jiang et al., 2017). Differences between land and sea temperatures can influence local wind patterns in coastal areas, creating situations where pollutants emitted overnight or in the morning and blown out to sea are recirculated back over (or near) the source area with a developing sea breeze (Yimin and Lyons, 2003; Levy et al., 2008). Such effects were not accounted for in our study but have been the focus of other research that have used recirculation metrics (Di Bernardino et al., 2022; Wang et al., 2022).

The large distances and sparse network in our data also means that there was a low chance of any particular AQS being downwind from a fire. This is indicated by the wind direction variables being clustered around zero (i.e. smoke not blowing from fire to AQS, see Fig. 3) and in cases such as Appendix A Fig. A3, where only two from > 20 AQS detected the smoke from a WF. It may therefore be that the models were mostly optimising for non-smoke-related $PM_{2.5}$, so it is not surprising that peak events are under-predicted. Our approach is promising, however, more data capturing individual fires burning near monitoring stations is likely required to produce better models. More data could be gathered from the same AQS for another analysis in the future, or by increasing the density of $PM_{2.5}$ monitors, either through installing more permanent AQS or via a short-term project that installs a network of temporary AQS in a selected fire-prone area (e.g. Blue Mountains) in times of high-expected fire activity.

Some of the variables had interesting non-linear effects. For example, wind speed at the fire during the afternoon was associated with high $PM_{2.5}$ both when wind speed was < ~ 7 km h^{-1} and > ~ 15 km h^{-1} (Fig. 6). Such relationships are due to complex factors. For example, it may be that low wind speeds increase $PM_{2.5}$ because previously emitted smoke is more likely to linger, whereas high wind speeds mean that fires are more intense and produce more smoke and particulates. In other words, low wind speed increases smoke concentration at the receiver and high wind speed increases smoke production. The low wind speed effect may be more associated with HRBs, which are conducted in calm weather, and the high wind speed effect associated with WFs. Similar non-linear relationships also exist for other variables, to varying degrees, including PBLH, RH, temperature and MSLP (Fig. 6). Some variables differed in their effects substantially between the fire and AQS. For example, afternoon PBLH at the fire showed increases in $PM_{2.5}$ at low and high levels, but at the AQS it was only low PBLH that increased $PM_{2.5}$. The PBLH effect at the fire may be similar to the wind effect: low PBLH traps smoke but high PBLH is associated with more active fire behaviour and greater smoke production. Note that there is uncertainty about the strength and

directions of the effects at the extremes of the predictor variables, given the lower proportion of observations for model training, as indicated in Figure 6.

Our models predict only small differences between $PM_{2.5}$ depending on the fire type variable (HRB or WF), which also had low permutation importance in all three models. Likely, the weather variables and fire area variables included in our model captured most of the differences between HRBs and WFs (e.g. WF on average are larger and burn in hotter windier weather), making the fire type variable mostly redundant in the models. In this case, the models suggest that after accounting for weather and fire size, there are no clear differences in WFs and HRBs in terms of $PM_{2.5}$ output. However, other studies have indicated that fundamental differences may exist as WFs inject smoke higher into the atmosphere and consume more fuel per hectare than HRBs (Price et al., 2022; Price et al., 2018; Volkova et al., 2014), thus WF and HRB differences need more investigation.

Our third aim was to ***make inferences about potential changes in HRB protocols that could reduce PM_{2.5} impacts.*** The models indicate the potential combinations of environmental and fire conditions where $PM_{2.5}$ is likely to be higher and fire managers must carefully consider whether to undertake HRBs due to $PM_{2.5}$ pollution risk. For example, a large HRB < 20 km from a town where PBLH < 300 m during the night and morning (at both fire and receiver site) and < 800 m during the afternoon. When HRBs are > 50 km from a town, a high $PM_{2.5}$ impact is much less likely, although certainly still possible (Appendix A). In addition, the HRB area should be a strong consideration as $PM_{2.5}$ is predicted to increase as daily active fire area increases between 0 and 2500 ha, although there is uncertainty at larger fire areas because few fires in our data were > 2500 ha (most were < 1000 ha). Note that our fire areas may be an underestimate of total HRB size, as these areas are calculated from VIIRS hotspots, thus based on active fire area at VIIRS overpass times (early afternoon and early mornings), not the total area burnt in a day.

While the models indicate that certain combinations of weather increase $PM_{2.5}$, this must be weighed with the fact that aspects of HRB implementation cannot always be changed. For example, HRBs are already conducted within the narrow set of weather conditions that allow for ignition and controllable fire spread and often need to be conducted close to populations to have the greatest house protection effect (Clarke et al., 2019). Due to the complex effects and lower predictive accuracy for HRBs, it is difficult to make precise predictions from the models for individual fires. A more detailed model would be required to identify the weather conditions that would allow an HRB to be safely conducted and also for $PM_{2.5}$ to be low. An assessment that combines predictions from our model of lower-risk $PM_{2.5}$ days with a model that predicts the occurrence of within-prescription HRB burning days (Clarke et al., 2019) may be useful to assess the number of overlapping days, i.e. HRB days with low $PM_{2.5}$ risk. The effects of different burning strategies, such as breaking a large burn up into multiple blocks, are unknown and could potentially worsen $PM_{2.5}$. Here we did not assess different strategies, and only analysed cases where one fire was burning at a time, not when multiple fires were burning around the same AQS at once. This is a significant limitation of the study, as the smokiest HRB days likely occur when multiple fires are burning at once and/or fires burn for longer periods. Price and Forehead (2021) also suggested overnight burning may have led to the largest $PM_{2.5}$ exceedances that they recorded using low-cost monitors near HRBs. Pearce et al. (2012) found burn duration to be an important predictor during their work also

monitoring $PM_{2.5}$ close to HRBs. The effect of total fire load in a region, i.e. total area of all fires, and regional weather conditions was the subject of separate research (Storey and Price, 2022).

5. Conclusion

540 Understanding how individual fires, both wildfires and hazard reduction burns, influence ambient $PM_{2.5}$ concentrations is important to allow for proper risk analysis, burn scheduling and issuance of warnings. Our models provide important insights into the influence of weather and fire variables on $PM_{2.5}$ concentration from individual fires. We found that daily active fire area, PBLH, temperature and RH all have strong influences, with the effects of the variables varying depending on whether it is measured at the fire site or the receiver location (here, the AQS). The models improve our understanding and may have a

545 place during operational predictions. However, accuracy is similar to existing models, so could be used as a complement. Further development to improve accuracy would benefit the operational deployment of the models, particularly given the lower correlations between observations and predictions for HRBs. However, our approach is promising and would likely produce better models with a larger set of data, where more cases of single fires near AQS could be found. Increasing the density of $PM_{2.5}$ monitors (permanent or temporary during fire seasons) would also provide better data to improve the resulting models.

550 Producing broader scale models of regional level $PM_{2.5}$ from regional level fire and weather may be a useful alternative approach for producing operational models.

555

560

565

6. Appendix A

This appendix contains case studies of large $PM_{2.5}$ exceedance events present in the data used for modelling in the main text. The purpose is to detail specific events and highlight factors that may have influenced $PM_{2.5}$ patterns across the different AQS. The appendix is organised as seven panel figures of seven different events that each have images and a description. The events

575 selected are the six highest mean 6-hour values from the combinations of fire type (WF, HRB) and period (afternoon, evening, morning), and also the second highest value for afternoon WF, which is included to highlight interesting coastal wind behaviour. Note that the values used in modelling are from AQS data for which only one fire was active within 150 km of the AQS for that day. Higher values were recorded on days with multiple fires, but these are not analysed in this paper. Each figure contains:

580 • Panel (a) in each figure has a background Himawari 8 satellite image for one single hour (time in black text at top) during the relevant time period, with the fire centroid also indicated by an orange circle and general fire area in blue polygon. The background image is overlaid with wind speed (red numbers and red arrow length) and wind direction (red arrow direction) from Bureau of Meteorology weather stations and $PM_{2.5}$ recorded at all AQS within the image extent at that hour (black circles and white text, larger $PM_{2.5}$ value means large circle). The AQS with the highest

585 mean six-hour value is indicated by a red star (same AQS as general location map in panel b). AQS that had multiple fires nearby are not included. Note one extra Himawari image is included for WF night to aid in the description (panel e). Himawari images are provided by Japan Aerospace Exploration Agency (JAXA) and were downloaded from the JAXA P-Tree System (https://www.eorc.jaxa.jp/ptree/terms.html).

• Panel (b) in each figure is a map of the general fire location, represented by an orange circle around the fire

590 centroid, with circles representing AQS locations coloured by their mean $PM_{2.5}$ value (μgm^{-3}) for that six-hour period. The highest station values are indicated by the red text and red star.

• Panels (c) and (d) in each figure are 10 m and 700 hPa gridded wind speed and direction for the same hour as the Himawari image, sampled from ERA5 gridded reanalysis data. Black arrows indicate wind speed and direction, with longer/larger arrows indicating higher wind speed. The orange fire circle is also in these images for reference.

595 The black solid line is the Australian coastline.

Fig. A1: Wildfire afternoon

The largest afternoon mean WF $PM_{2.5}$ was 294.2 μgm^{-3} at Katoomba AQS, which was the third closest to fire. The fire (Gosper's Mountain) eventually burnt ~ 500,000 ha. 15 other AQS around the fire had mean $PM_{2.5} > 50$. The smoke was flowing mainly to the south over Katoomba (red star) under the surface northerly winds. However, a portion of the smoke was also flowing more easterly with upper-level winds. There is a distinct easterly edge to the smoke plume (a), which appears to align with where the northerly and north-easterly surface winds. There were widespread $PM_{2.5}$ exceedances but only Katoomba recorded values > 150 μgm^{-3} (b). Smoke from other wildfires to the north of Sydney may have affected the region, indicated by the AQS north of the Gosper's fire also recording high $PM_{2.5}$ values (a). These AQS are not shown in (b) because they were within 150 km of more than one active fire. In the morning before this image, smoke was flowing directly into Sydney and most AQS recorded at least one hourly value > 200 μgm^{-3}.

Fig. A2: Wildfire afternoon 2

The second highest mean afternoon WF $PM_{2.5}$ was 138.1 μgm^{-3} at Richmond AQS (red star), which was the closest to the fire at ~50 km. This was also the Gosper's Mountain fire. Six other AQS in the Sydney basin had mean $PM_{2.5} > 50$ (b). The smoke flow appears multidirectional (a): to the south with surface winds (c) and to the east with upper-level winds (d). The southerly flow appears to be due to the meeting of surface westerly winds and a NE sea breeze (c). The smoke flowing to the east appears to be above the surface and above the sea breeze as the AQS directly to the east of the fire was under the plume but only recording $PM_{2.5}$ of 7 μgm^{-3} (a). The morning preceding had northerly winds blowing smoke directly into Sydney, with several AQS recording hourly values in the 100s, so lingering smoke was likely a contributor. This fire burnt through the following night but $PM_{2.5}$ levels dropped substantially across Sydney (all < 25 μgm^{-3}) until 2am, when $PM_{2.5}$ increased again (Fig. A4).
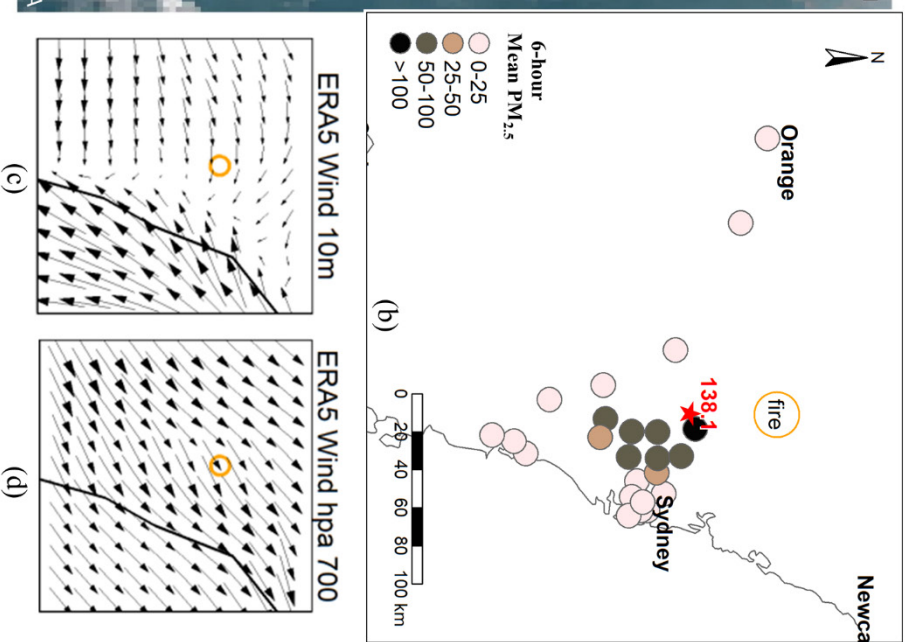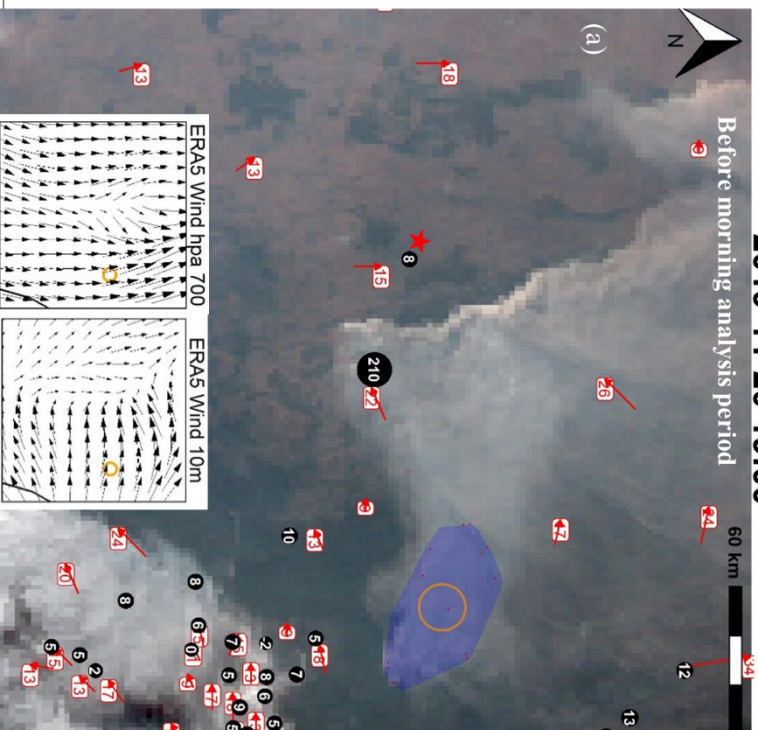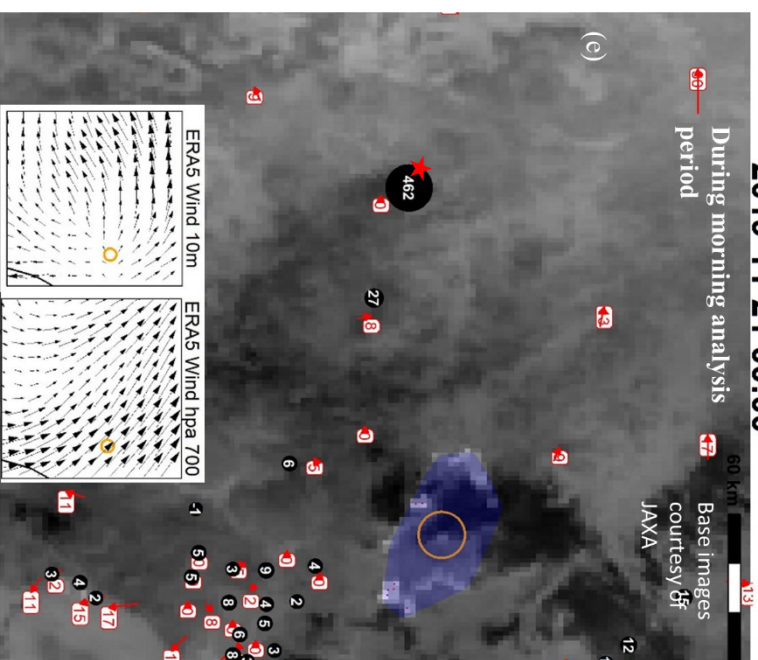
Fig. A3: Wildfire night. The highest mean night WF PM$_{2.5}$ was 394.8 µgm^{-3} at Orange (red star), also from the Gosper's Mountain fire. All except one other AQS (Bathurst 25-50 µgm^{-3}) had mean PM$_{2.5}$ < 25 µgm^{-3} for this period (b). At midnight (e) the smoke appears to be flowing directly from the fire to Orange (PM2.5 = 462 µgm^{-3}), given no AQS in Sydney (SE of fire) had high PM$_{2.5}$, and there were easterly 10 m winds (f). This example shows that smoke circulation can be complex. At 19:00, one hour before our "night" period here, there were easterlies at the fire but Orange AQS had southerlies (a). The easterlies had only reached Bathurst (PM$_{2.5}$=210 µgm^{-3}) and not Orange (PM$_{2.5}$=8 µgm^{-3}). Later (e) the easterlies reached Orange along with the surface smoke, resulting in high PM$_{2.5}$. In the day after this, winds switched to northerlies and PM$_{2.5}$ rose substantially across Sydney and in Katoomba.
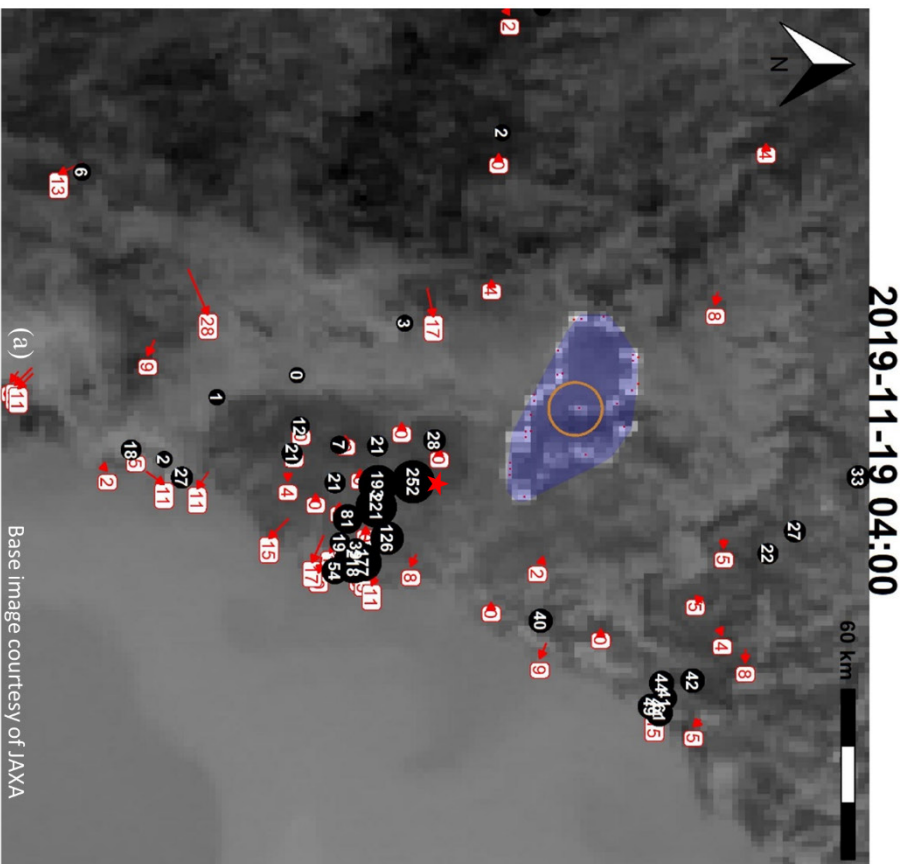
Fig. A4: Wildfire morning
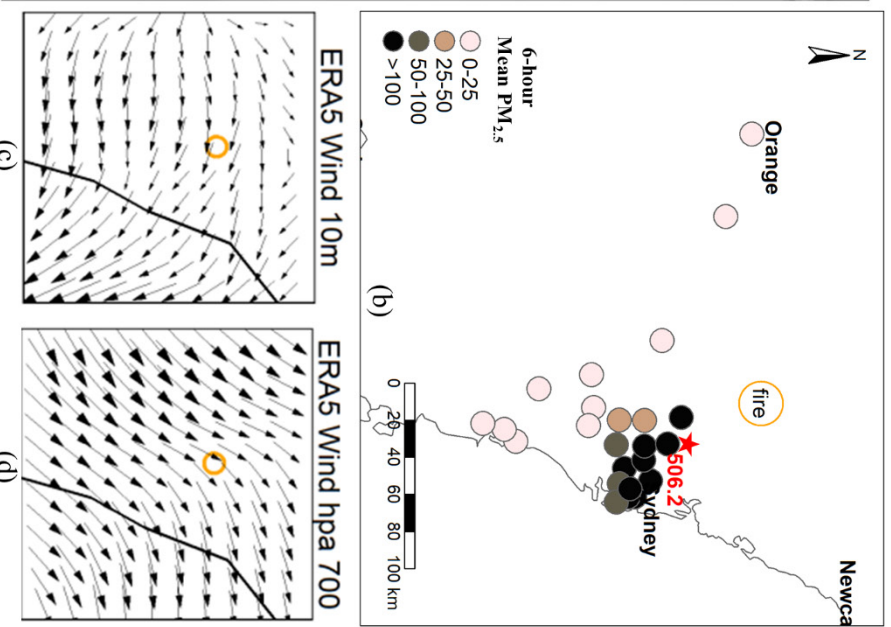
The highest mean morning WF $PM_{2.5}$ was 506.2 µgm⁻³ at Rouse Hill (red star), which was the second closest AQS at 30-40 km from the fire. This was also the Gosper's Mountain fire. Richmond AQS was closer but recorded mean $PM_{2.5}$ of 112 µgm⁻³. There were seven other AQS with a mean > 100 µgm⁻³ for this period and another three > 50 µgm⁻³ (b). It is not apparent from the BOM wind (red arrows in a) or the ERA5 data (c and d) that wind flowed directly from the fire to Rouse Hill. The high values may be the result of smoke lingering from the previous day (Fig. A2). However, smoke appeared to clear out during the night period preceding this morning, as the night had comparatively low $PM_{2.5}$ values (all Sydney AQS < 25 µgm⁻³). There may have been drainage flows from the mountains into the Sydney basin that were not captured in the weather data. After this morning, winds turned westerly then southerly, which pushed smoke away from Sydney and reduced $PM_{2.5}$ < 25 µgm⁻³ across Sydney.

600
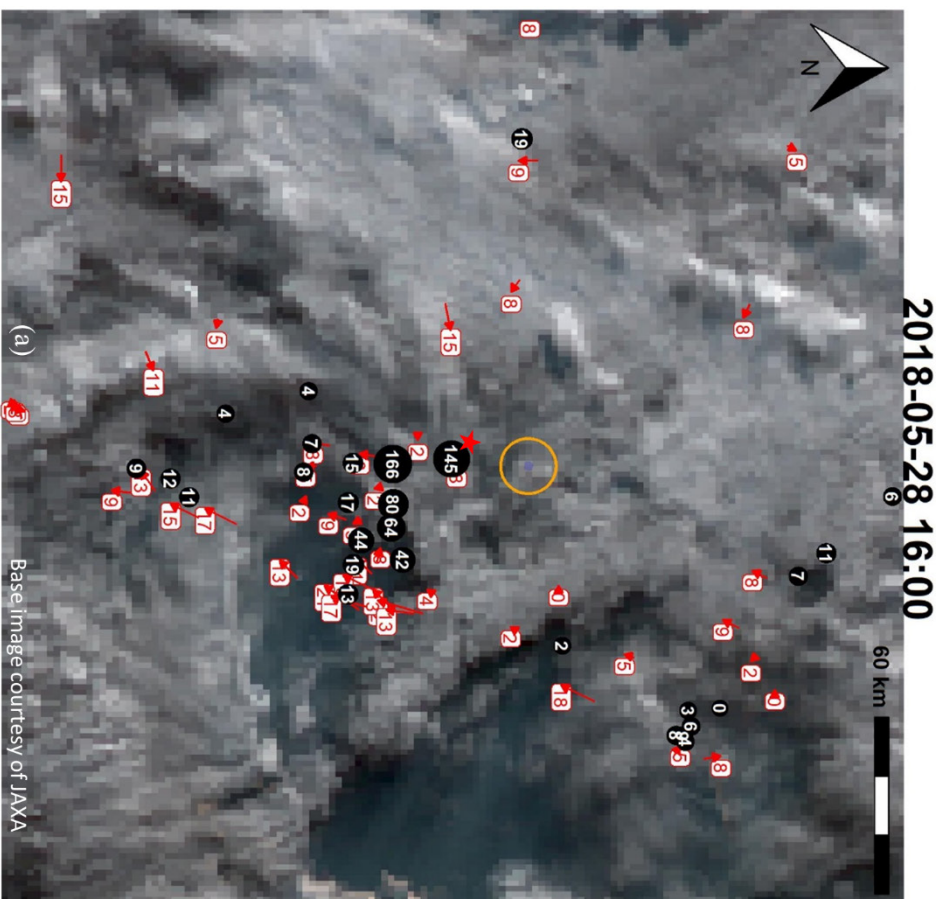
Fig. A5: HRB afternoon

The highest mean afternoon HRB PM$_{2.5}$ was 145.9 μgm^{-3} at the closest AQS in Richmond (red star). Four other AQS also recorded PM$_{2.5}$ > 50 μgm^{-3} during the same period (b). Wind patterns at 10 m (c) suggest that the northerly winds and the meeting of NW and NE winds to the west of the fire funnelled surface smoke to Sydney, similar to Fig. A2. Wind speeds were also low (a and c), meaning smoke would have remained in the area for longer. On the morning preceding this period, there was likely some smoke lingering around Sydney because several AQS recorded hourly values in the 20s and 30s (μgm^{-3}). The synoptic wind direction (d) in the afternoon was northerly, meaning high-level smoke would also have flowed toward Sydney. PM$_{2.5}$ continued to increase as the day went on and into the night. The highest night mean PM$_{2.5}$ was also caused by this HRB (Fig. A6).
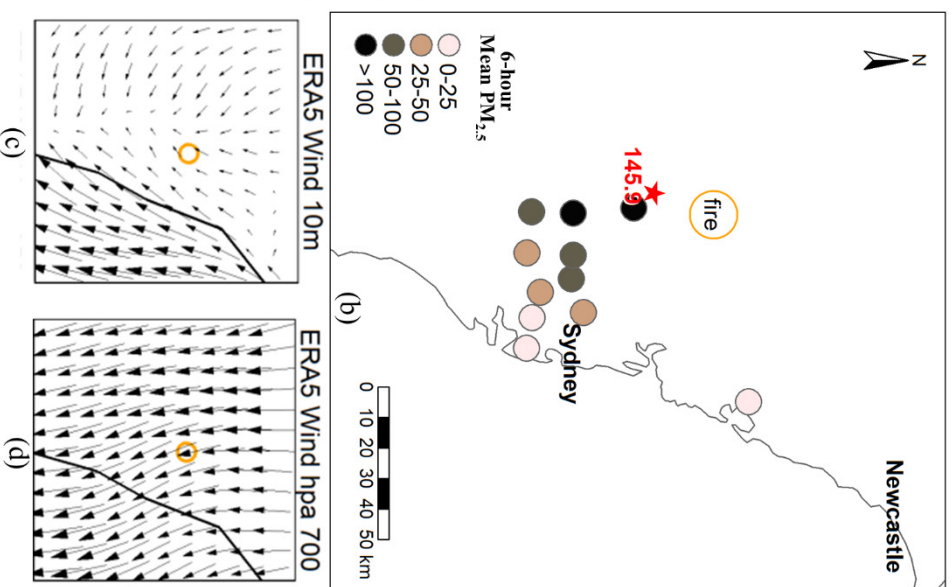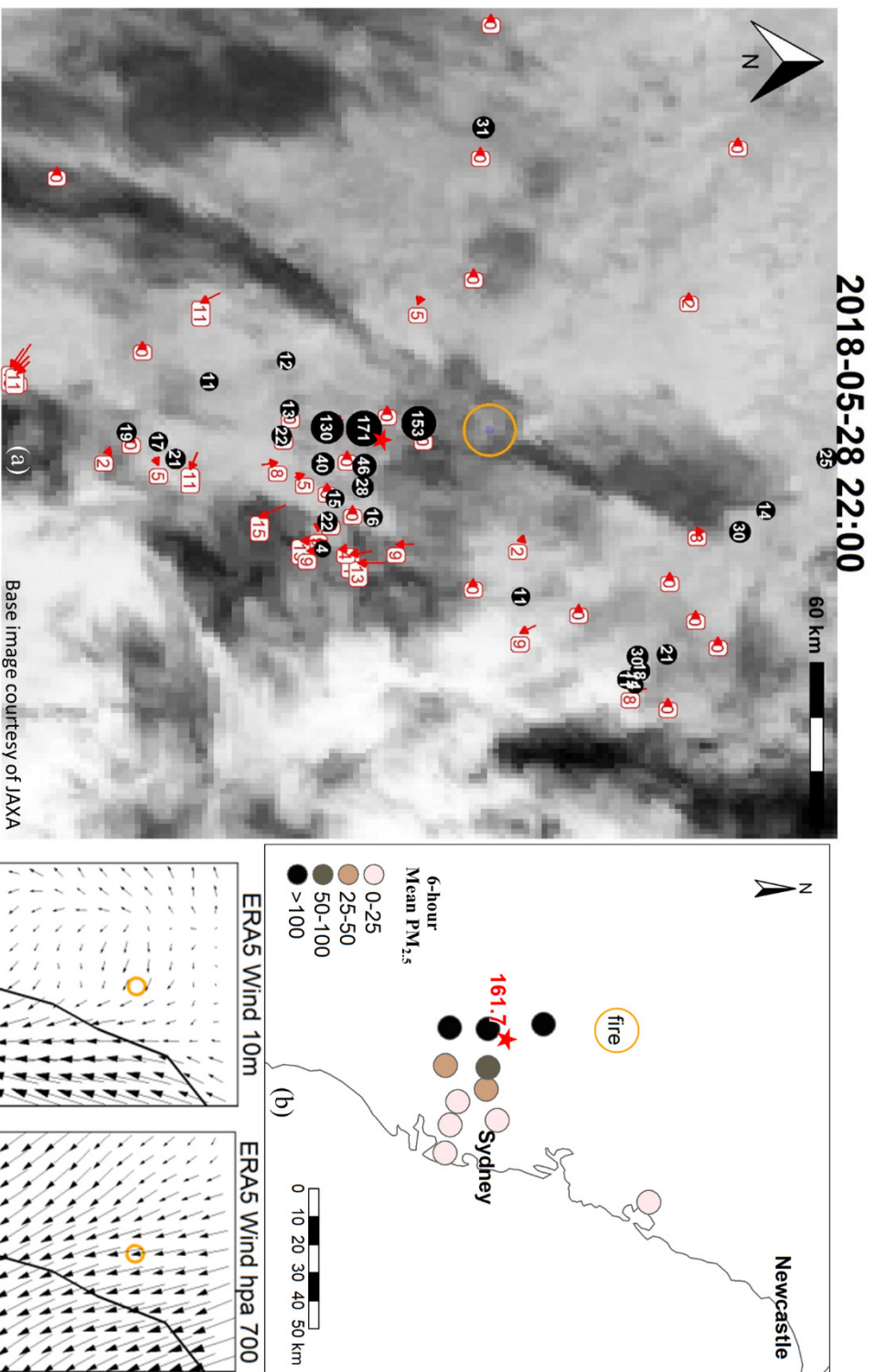
Fig. A6: HRB night

The highest mean night HRB PM$_{2.5}$ was 161.7 μgm^{-3} at the second closest AQS in St Marys (red star), while the closest station was also high (Richmond = 129.4 μgm^{-3}). This highest night-time PM$_{2.5}$ for HRBs followed the highest afternoon PM$_{2.5}$ for the fire (Fig. A5). The high afternoon PM$_{2.5}$ may have influenced the results this night as 10 m winds were still low (c), suggesting smoke may have lingered from the afternoon. Low wind speeds also meant that any new smoke produced during the night was probably not dispersed. The 10 m winds (c) suggest smoke was not flowing directly from the fire to St Marys, as winds were westerly at the fire. However, the BOM winds (red arrows in a) are zero at Richmond and St Marys at 22:00, suggesting very calm conditions.

2018-05-28 22:00

Base image courtesy of JAXA

60 km

ERA5 Wind 10m (c)

ERA5 Wind hpa 700 (d)

6-hour Mean PM$_{2.5}$
● 0-25
● 25-50
● 50-100
○ >100

fire

161.7

Sydney

Newcastle

0 10 20 30 40 50 km

(b)
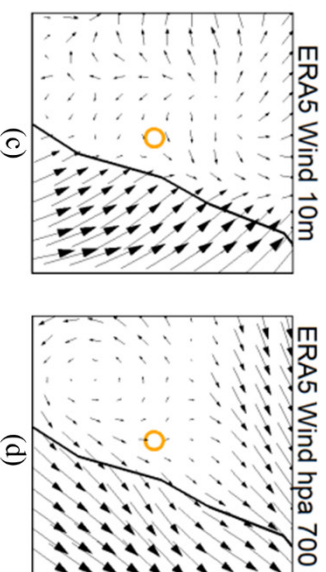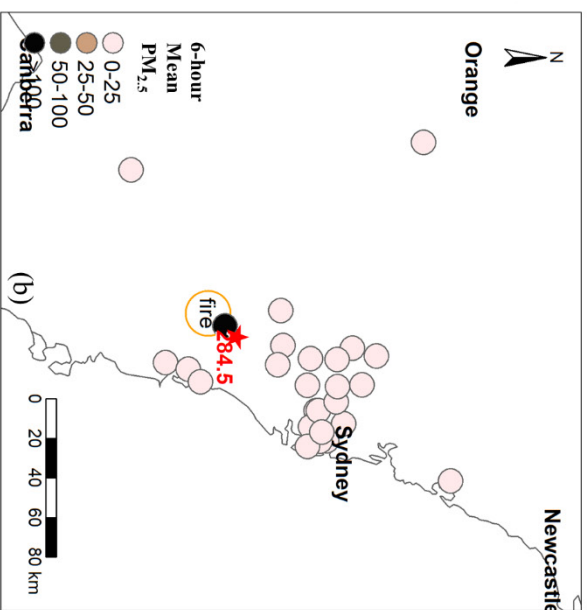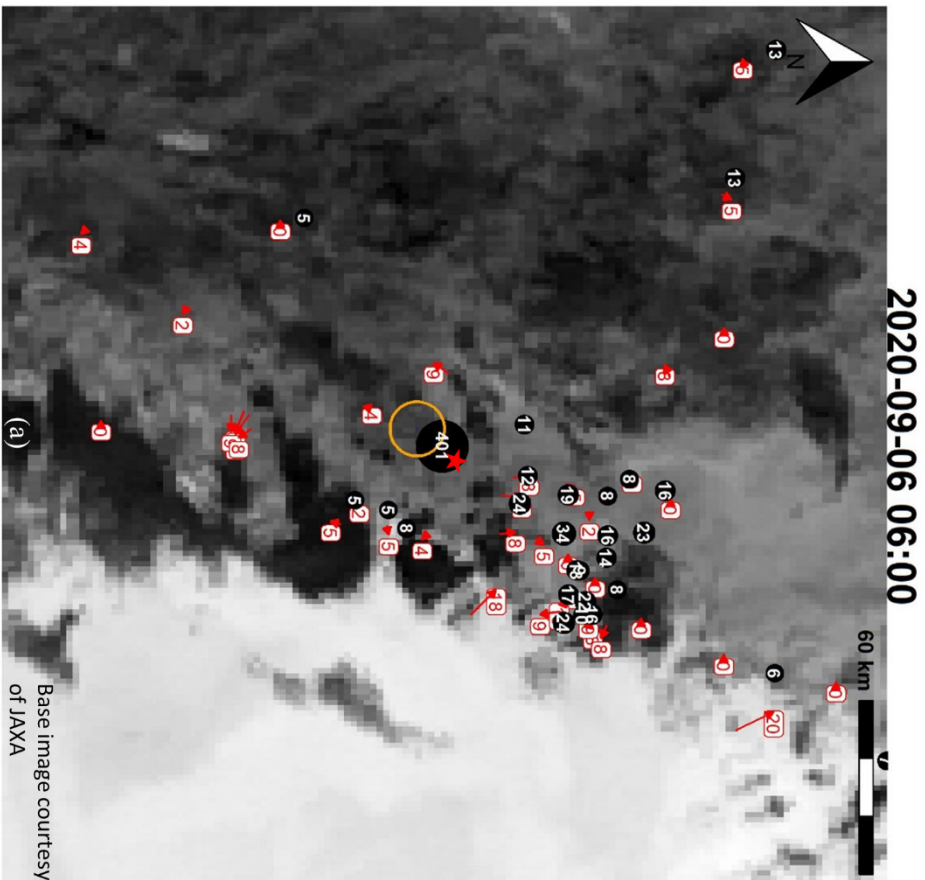
Fig. A7: HRB morning

The highest mean morning HRB PM$_{2.5}$ was 284.5 μgm^{-3} at Bargo AQS (red star) 10 km from the HRB. This example differs to the other panels in that the PM$_{2.5}$ impact was local only: no other AQS were > 25 μgm^{-3} for this morning (b). None of the examples (Fig. A1-A6) had AQS at such a close distance. The 10 m winds (c) suggest light winds from the north toward the fire toward the AQS. The BOM winds near the fire (a) varied in direction but were light. The wind speeds were likely too low to carry smoke far enough north to impact AQS in Sydney or AQS in other directions. This HRB was ignited the previous day under W/SW winds but did not noticeably increase PM$_{2.5}$ at Bargo until the day after this morning period, strong northerly winds occurred and PM$_{2.5}$ at Bargo dropped below 10 μgm^{-3}.

7. Author Contributions

605 Owen Price developed the research aims. Michael Storey and Owen Price developed the analysis method. Michael Storey ran the statistical analysis and wrote the manuscript. Owen Price edited the manuscript.

8. Data Availability

VIIRS SNPP hotspots used for analysis are freely available via the NANA FIRMS website at https://firms.modaps.eosdis.nasa.gov/download/

610 New South Wales $PM_{2.5}$ data are freely available from the New South Wales Government at free online at https://data.airquality.nsw.gov.au/docs/index.html.

Information on ERA5 gridded reanalysis weather product download is at https://www.ecmwf.int/en/forecasts/datasets/reanalysis-datasets/era5

9. Acknowledgements

615 This research was funded by the NSW Department of Planning, Industry and Environment, via the NSW Bushfire Risk Management Research Hub.

The results contain modified Copernicus Climate Change Service information 2021. Neither the European Commission nor ECMWF is responsible for any use that may be made of the Copernicus information or data it contains.

10. Competing interests

620 The authors declare that they have no conflict of interest.

11. References

Biau, G. and Scornet, E.: A random forest guided tour, TEST, 25, 197-227, 10.1007/s11749-016-0481-7, 2016.

Boer, M. M., Resco de Dios, V., and Bradstock, R. A.: Unprecedented burn area of Australian mega forest fires, Nature Climate Change, 10, 171-172, 10.1038/s41558-020-0716-1, 2020.

625 Borchers-Arriagada, N., Bowman, D. M. J. S., Price, O., Palmer, A. J., Samson, S., Clarke, H., Sepulveda, G., and Johnston, F. H.: Smoke health costs change the calculus for wildfires fuel management, The Lancet Planetary Health, 5, E608-E619, 2021.

Bradshaw, S. D., Dixon, K. W., Lambers, H., Cross, A. T., Bailey, J., and Hopper, S. D.: Understanding the long-term impact of prescribed burning in mediterranean-climate biodiversity hotspots, with a focus on south-western Australia, International Journal of Wildland Fire, 27, 643-657, 10.1071/wf18067, 2018.

630 Broome, R. A., Johnstone, F. H., Horsley, J., and Morgan, G. G.: A rapid assessment of the impact of hazard reduction burning around Sydney, May 2016, Medical Journal of Australia, 205, 407-408, 10.5694/mja16.00895, 2016.

Chen, G., Guo, Y., Yue, X., Tong, S., Gasparrini, A., Bell, M. L., Armstrong, B., Schwartz, J., Jaakkola, J. J. K., Zanobetti, A., Lavigne, E., Nascimento Saldiva, P. H., Kan, H., Royé, D., Milojevic, A., Overcenco, A., Urban, A., Schneider, A., Entezari, A., Vicedo-Cabrera, A. M., Zeka, A., Tobias, A., Nunes, B., Alahmad, B., Forsberg, B., Pan, S.-C., Íñiguez, C., Ameling, C., De la Cruz Valencia, C., Åström, C., Houthuijs, D., Van Dung, D., Samoli, E., Mayvaneh, F., Sera, F., Carrasco-Escobar, G., Lei, Y., Orru, H., Kim, H., Holobaca, I.-H., Kyselý, J., Teixeira, J. P., Madureira, J., Katsouyanni, K., Hurtado-Díaz, M., Maasikmets, M., Ragettli, M. S., Hashizume, M., Stafoggia, M., Pascal, M., Scortichini, M., de Sousa Zanotti Stagliorio Coêlho, M., Valdés Ortega, N., Ryti, N. R. I., Scovronick, N., Matus, P., Goodman, P., Garland, R. M., Abrutzky, R., Garcia, S. O., Rao, S., Fratianni, S., Dang, T. N., Colistro, V., Huber, V., Lee, W., Seposo, X., Honda, Y., Guo, Y. L., Ye, T., Yu, W., Abramson, M. J., Samet, J. M., and Li, S.: Mortality risk attributable to wildfire-related PM2.5 pollution: a global time series study in 749 locations, The Lancet Planetary Health, 5, e579-e587, 10.1016/S2542-5196(21)00200-X, 2021.

Clarke, H., Tran, B., Boer, M. M., Price, O., Kenny, B., and Bradstock, R.: Climate change effects on the frequency, seasonality and interannual variability of suitable prescribed burning weather conditions in south-eastern Australia, Agricultural and Forest Meteorology, 271, 148-157, https://doi.org/10.1016/j.agrformet.2019.03.005, 2019.

Cope, M., Keywood, M., Emmerson, K., Galbally, I., Boast, K., Chambers, S., Cheng, M., Crumeyrolle, S., Dunne, E., and Fedele, R.: Sydney particle study-stage-II, CSIRO Marine and Atmospheric Research2014.

Di Bernardino, A., Iannarelli, A. M., Casadio, S., Pisacane, G., Mevi, G., and Cacciani, M.: Classification of synoptic and local-scale wind patterns using k-means clustering in a Tyrrhenian coastal area (Italy), Meteorology and Atmospheric Physics, 134, 30, 10.1007/s00703-022-00871-z, 2022.

Di Virgilio, D., Hart, M. A., and Jiang, N.: Meteorological controls on atmospheric particulate pollution during hazard reduction burns, Atmospheric Chemistry and Physics, 18, 6585–6599, 2018a.

Di Virgilio, G., Hart, M. A., and Jiang, N.: Meteorological controls on atmospheric particulate pollution during hazard reduction burns, Atmos. Chem. Phys., 18, 6585-6599, 10.5194/acp-18-6585-2018, 2018b.

Emery, C., Liu, Z., Russell, A. G., Odman, M. T., Yarwood, G., and Kumar, N.: Recommendations on statistics and benchmarks to assess photochemical model performance, Journal of the Air & Waste Management Association, 67, 582-598, 10.1080/10962247.2016.1265027, 2017.

Filkov, A. I., Ngo, T., Matthews, S., Telfer, S., and Penman, T. D.: Impact of Australia's catastrophic 2019/20 bushfire season on communities and environment. Retrospective analysis and current trends, Journal of Safety Science and Resilience, 1, 44-56, https://doi.org/10.1016/j.jnlssr.2020.06.009, 2020.

Fine, P. M., Sioutas, C., and Solomon, P. A.: Secondary Particulate Matter in the United States: Insights from the Particulate Matter Supersites Program and Related Studies, Journal of the Air & Waste Management Association, 58, 234-253, 10.3155/1047-3289.58.2.234, 2008.

Gill, T.: Woody vegetation cover - Landsat, JRSRP, Australian coverage, 2000-2010. (Version 1.0.0.), Terrestrial Ecosystem Research Network. [dataset], 2012.

Gill, T., Johansen, K., Phinn, S., Trevithick, R., Scarth, P., and Armston, J.: A method for mapping Australian woody vegetation cover by linking continental-scale field data and long-term Landsat time series, International Journal of Remote Sensing, 38, 679-705, 10.1080/01431161.2016.1266112, 2017.

Greenwell, B. M.: pdp: an R Package for constructing partial dependence plots, The R Journal, 9, 421, 2017.

Gupta, P., Christopher, S. A., Box, M. A., and Box, G. P.: Multi year satellite remote sensing of particulate matter air quality over Sydney, Australia, International Journal of Remote Sensing, 28, 4483-4498, 10.1080/01431160701241738, 2007.

Haikerwal, A., Akram, M., Sim, M. R., Meyer, M., Abramson, M. J., and Dennekamp, M.: Fine particulate matter (PM2.5) exposure during a prolonged wildfire period and emergency department visits for asthma, Respirology, 21, 88-94, 10.1111/resp.12613, 2016.

Hart, M., De Dear, R., and Hyde, R.: A synoptic climatology of tropospheric ozone episodes in Sydney, Australia, International Journal of Climatology, 26, 1635-1649, 10.1002/joc.1332, 2006.

He, C. R., Miljevic, B., Crilley, L. R., Surawski, N. C., Bartsch, J., Salimi, F., Uhde, E., Schnelle-Kreis, J., Orasche, J., Ristovski, Z., Ayoko, G. A., Zimmermann, R., and Morawska, L.: Characterisation of the impact of open biomass burning on urban air quality in Brisbane, Australia, Environment International, 91, 230-242, 10.1016/j.envint.2016.02.030, 2016.

ERA5 hourly data on pressure levels from 1979 to present: 10.24381/cds.bd0915c6, last access: 2021.

ERA5 hourly data on single levels from 1979 to present: 10.24381/cds.adbb2d47, last access: 2021.

Hu, X., Belle, J. H., Meng, X., Wildani, A., Waller, L. A., Strickland, M. J., and Liu, Y.: Estimating PM2.5 Concentrations in the Conterminous United States Using the Random Forest Approach, Environmental Science & Technology, 51, 6936-6944, 10.1021/acs.est.7b01210, 2017.

Jaffe, D., Hafner, W., Chand, D., Westerling, A., and Spracklen, D.: Interannual Variations in PM2.5 due to Wildfires in the Western United States, Environmental Science & Technology, 42, 2812-2818, 10.1021/es702755v, 2008.

Jiang, N., Scorgie, Y., Hart, M., Riley, M. L., Crawford, J., Beggs, P. J., Edwards, G. C., Chang, L., Salter, D., and Virgilio, G. D.: Visualising the relationships between synoptic circulation type and air quality in Sydney, a subtropical coastal-basin environment, 37, 1211-1228, https://doi.org/10.1002/joc.4770, 2017.

Johnston, F. H., Borchers-Arriagada, N., Morgan, G. G., Jalaludin, B., Palmer, A. J., Williamson, G. J., and Bowman, D. M. J. S.: Unprecedented health costs of smoke-related PM2.5 from the 2019–20 Australian megafires, Nature Sustainability, 4, 42-47, 10.1038/s41893-020-00610-5, 2021.

690 Johnston, F. H., Henderson, S. B., Chen, Y., Randerson, J. T., Marlier, M., DeFries, R. S., Kinney, P., Bowman, D., and Brauer, M.: Estimated Global Mortality Attributable to Smoke from Landscape Fires, Environmental Health Perspectives, 120, 695-701, 10.1289/ehp.1104422, 2012.

Levy, I., Dayan, U., and Mahrer, Y.: A five-year study of coastal recirculation and its effect on air pollutants over the East Mediterranean region, Journal of Geophysical Research: Atmospheres, 113, https://doi.org/10.1029/2007JD009529, 2008.

695 Matz, C. J., Egyed, M., Xi, G., Racine, J., Pavlovic, R., Rittmaster, R., Henderson, S. B., and Stieb, D. M.: Health impact analysis of PM2.5 from wildfire smoke in Canada (2013–2015, 2017–2018), Science of The Total Environment, 725, 138506, https://doi.org/10.1016/j.scitotenv.2020.138506, 2020.

Miller, C., O'Neill, S., Rorig, M., and Alvarado, E.: Air-Quality Challenges of Prescribed Fire in the Complex Terrain and Wildland Urban Interface Surrounding Bend, Oregon, Atmosphere, 10, 10.3390/atmos10090515, 2019.

700 Fire Information for Resource Management System (FIRMS): https://earthdata.nasa.gov/earth-observation-data/near-real-time/firms, last NPWS Fire History - Wildfires and Prescribed Burns

 https://datasets.seed.nsw.gov.au/dataset/fire-history-wildfires-and-prescribed-burns-1e8b6, last

Pearce, J. L., Rathbun, S., Achtemeier, G., and Naeher, L. P.: Effect of distance, meteorology, and burn attributes on ground-level particulate matter emissions from prescribed fires, Atmospheric Environment, 56, 203-211, 10.1016/j.atmosenv.2012.02.056, 2012.

705 Price, O. F. and Bradstock, R. A.: The spatial domain of wildfire risk and response in the Wildland Urban Interface in Sydney, Australia, Natural Hazards and Earth System Sciences, 13, 3385-3393, 2013.

Price, O. F. and Forehead, H.: Smoke patterns around prescribed fires in Australian eucalypt forests, as measured by low-cost particulate monitors, Atmosphere, 12, 1389, https://doi.org/10.3390/atmos12111389, 2021.

Price, O. F., Purdam, P. J., Williamson, G. J., and Bowman, D. M. J. S.: Comparing the height and area of wild and prescribed fire particle
710 plumes in south-east Australia using weather radar %J International Journal of Wildland Fire, 27, 525-537, https://doi.org/10.1071/WF17166, 2018.

Price, O. F., Williamson, G. J., Henderson, S. B., Johnston, F., and Bowman, D. M. J. S.: The Relationship between Particulate Pollution Levels in Australian Cities, Meteorology, and Landscape Fire Activity Detected from MODIS Hotspots, PLoS ONE, 7, e47327, 10.1371/journal.pone.0047327, 2012.

715 Price, O. H., Nolan, R. H., and Samson, S. A.: Fuel consumption rates in resprouting eucalypt forest during hazard reduction burns, cultural burns and wildfires, Forest Ecology and Management, 505, 119894, https://doi.org/10.1016/j.foreco.2021.119894, 2022.

Reid, C. E., Brauer, M., Johnston, F. H., Jerrett, M., Balmes, J. R., and Elliott, C. T.: Critical Review of Health Impacts of Wildfire Smoke Exposure, Environmental Health Perspectives, 124, 1334-1343, http://dx.doi.org/10.1289/ehp.1409277, 2016.

Reisen, F., Meyer, C. P., Weston, C. J., and Volkova, L.: Ground-Based Field Measurements of PM2.5 Emission Factors From Flaming
720 and Smoldering Combustion in Eucalypt Forests, Journal of Geophysical Research: Atmospheres, 123, 8301-8314, https://doi.org/10.1029/2018JD028488, 2018.

Reisen, F., Duran, S. M., Flannigan, M., Elliott, C., and Rideout, K.: Wildfire smoke and public health risk, International Journal of Wildland Fire, 24, 1029, 10.1071/wf15034, 2015.

Rodriguez-Galiano, V., Sanchez-Castillo, M., Chica-Olmo, M., and Chica-Rivas, M. J. O. G. R.: Machine learning predictive models for
725 mineral prospectivity: An evaluation of neural networks, random forest, regression trees and support vector machines, 71, 804-818, 2015.

Saide, P. E., Peterson, D. A., da Silva, A., Anderson, B., Ziemba, L. D., Diskin, G., Sachse, G., Hair, J., Butler, C., Fenn, M., Jimenez, J. L., Campuzano-Jost, P., Perring, A. E., Schwarz, J. P., Markovic, M. Z., Russell, P., Redemann, J., Shinozuka, Y., Streets, D. G., Yan, F., Dibb, J., Yokelson, R., Toon, O. B., Hyer, E., and Carmichael, G. R.: Revealing important nocturnal and day-to-day variations in fire smoke emissions through a multiplatform inversion, Geophysical Research Letters, 42, 3609-3618, 10.1002/2015gl063737, 2015.

730 Schroeder, W., Oliva, P., Giglio, L., and Csiszar, I. A.: The New VIIRS 375m active fire detection data product: Algorithm description and initial assessment, Remote Sensing of Environment, 143, 85-96, https://doi.org/10.1016/j.rse.2013.12.008, 2014.

Shah, S. U., Yebra, M., Van Dijk, A. I. J. M., and Cary, G. J.: A New Fire Danger Index Developed by Random Forest Analysis of Remote Sensing Derived Fire Sizes, 5, 152, 2022.

Specht, R. L. and Specht, A.: Australian plant communities: dynamics of structure, growth and biodiversity, Oxford University Press1999.

735 Storey, M. A. and Price, O. F.: Prediction of air quality in Sydney, Australia as a function of forest fire load and weather using Bayesian statistics, PLOS ONE, 17, e0272774, 10.1371/journal.pone.0272774, 2022.

Strobl, C., Boulesteix, A.-L., Kneib, T., Augustin, T., and Zeileis, A.: Conditional variable importance for random forests, BMC Bioinformatics, 9, 307, 10.1186/1471-2105-9-307, 2008.

Volkova, L., Meyer, C. P. M., Murphy, S., Fairman, T., Reisen, F., and Weston, C.: Fuel reduction burning mitigates wildfire effects on
740 forest carbon and greenhouse gas emission %J International Journal of Wildland Fire, 23, 771-780, https://doi.org/10.1071/WF14009, 2014.

Wang, T., Du, H., Zhao, Z., Russo, A., Zhang, J., and Zhou, C.: The impact of potential recirculation on the air quality of Bohai Bay in China, Atmospheric Pollution Research, 13, 101268, https://doi.org/10.1016/j.apr.2021.101268, 2022.

Wright, M. and Ziegler, A.: ranger: A Fast Implementation of Random Forests for High Dimensional Data in C++ and R., Journal of Statistical Software, 77, 1-17, 10.18637/jss.v077.i01, 2017.

Wright, M. N., Ziegler, A., and König, I. R.: Do little interactions get lost in dark random forests?, BMC Bioinformatics, 17, 145, 10.1186/s12859-016-0995-8, 2016.

Yao, J., Brauer, M., and Henderson, S. B.: Evaluation of a Wildfire Smoke Forecasting System as a Tool for Public Health Protection, Environmental Health Perspectives, 121, 1142-1147, 2014.

Yimin, M. and Lyons, T. J.: Recirculation of coastal urban air pollution under a synoptic scale thermal trough in Perth, Western Australia, Atmospheric Environment, 37, 443-454, https://doi.org/10.1016/S1352-2310(02)00926-3, 2003.

Zeng, T., Wang, Y. H., Yoshida, Y., Tian, D., Russell, A. G., and Barnard, W. R.: Impacts of Prescribed Fires on Air Quality over the Southeastern United States in Spring Based on Modeling and Ground/Satellite Measurements, Environmental Science & Technology, 42, 8401-8406, 10.1021/es800363d, 2008.